LEVEL II

REPORT NO. NADC-77202-30
RE-587

14

EVALUATION OF DYNAMICALLY RIVETED JOINTS

by

Basil P. Leftheris+
H. Eidinoff*
and
R.E. Hooson*

Research Department
Grumman Aerospace Corporation
Bethpage, New York 11714

July 1979

Final Report

Contract No. N62269-77-C-0478

Approved for Public Release; Distribution Unlimited

Prepared for

Naval Air Development Center
Warminster, Pennsylvania 18974

+ Principal Investigator
* Grumman Engineering Department

NOTICES

REPORT NUMBERING SYSTEM - The numbering of technical project reports issued by the Naval Air Development Center is arranged for specific identification purposes. Each number consists of the Center acronym, the calendar year in which the number was assigned, the sequence number of the report within the specific calendar year, and the official 2-digit correspondence code of the Command Office or the Functional Directorate responsible for the report. For example: Report No. NADC-78015-20 indicates the fifteeth Center report for the year 1978, and prepared by the Systems Directorate. The numerical codes are as follows:

CODE	OFFICE OR DIRECTORATE
00	Commander, Naval Air Development Center
01	Technical Director, Naval Air Development Center
02	Comptroller
10	Directorate Command Projects
20	Systems Directorate
30	Sensors & Avionics Technology Directorate
40	Communication & Navigation Technology Directorate
50	Software Computer Directorate
60	Aircraft & Crew Systems Technology Directorate
70	Planning Assessment Resources
80	Engineering Support Group

PRODUCT ENDORSEMENT - The discussion or instructions concerning commercial products herein do not constitute an endorsement by the Government nor do they convey or imply the license or right to use such products.

APPROVED BY: Edward J. Stone DATE: 30 March 1979

UNCLASSIFIED

SECURITY CLASSIFICATION OF THIS PAGE (When Data Entered)

(19) REPORT DOCUMENTATION PAGE

READ INSTRUCTIONS BEFORE COMPLETING FORM

(12) 1. REPORT NUMBER: NADC-77202-30	2. GOVT ACCESSION NO.
3. RECIPIENT'S CATALOG NUMBER	
(6) 4. TITLE (and Subtitle): EVALUATION OF DYNAMICALLY RIVETED JOINTS.	(9) 5. TYPE OF REPORT & PERIOD COVERED: FINAL REPORT, 1 [illegible] - 30 [illegible]
(14) 6. PERFORMING ORG. REPORT NUMBER: RE-587	
(10) 7. AUTHOR(s): Basil P. Leftheris, H. Eidinoff, R. E. Hooson	(15) 8. CONTRACT OR GRANT NUMBER(s): N62269-77-C-0478
9. PERFORMING ORGANIZATION NAME AND ADDRESS: GRUMMAN AEROSPACE CORP. RESEARCH DEPT. BETHPAGE, N.Y. 11714 (16) F41-1	(17) 10. PROGRAM ELEMENT, PROJECT, TASK AREA & WORK UNIT NUMBERS: AIRTASK WF41-400-000 WORK UNIT ZA-101
11. CONTROLLING OFFICE NAME AND ADDRESS: Naval Air Development Center, Warminster, Pennsylvania 18974 (12) 71	(11) 12. REPORT DATE: Jul[illegible]79
	13. NUMBER OF PAGES: 66
14. MONITORING AGENCY NAME & ADDRESS (if different from Controlling Office)	15. SECURITY CLASS. (of this report): UNCLASSIFIED
	15a. DECLASSIFICATION/DOWNGRADING SCHEDULE

16. DISTRIBUTION STATEMENT (of this Report)

Approved for Public Release; Distribution Unlimited

17. DISTRIBUTION STATEMENT (of the abstract entered in Block 20, if different from Report)

18. SUPPLEMENTARY NOTES

19. KEY WORDS (Continue on reverse side if necessary and identify by block number)

Fastenings	Fatigue-Improvement Fasteners	Stress Wave Riveter
Fatigue	Interference Fit Fasteners	
Fatigue Life	Joints	
Fatigue Tests	Fastened Joints	
	Aluminum Joints	

20. ABSTRACT (Continue on reverse side if necessary and identify by block number)

The performance of stress wave driven rivet installations is evaluated in terms of crack growth arresting capability, using precracked specimens subjected to constant amplitude and spectrum fatigue loading. Rivets installed in pre-cracked holes using the Grumman Stress Wave Riveter (SWR) are shown to be effective in arresting crack growth. Residual stresses resulting from rivet coldwork are determined and the effective stress intensity factor, K_I, is calculated. It is concluded → over

DD FORM 1 JAN 73 1473 EDITION OF 1 NOV 65 IS OBSOLETE S/N 0102-014-6601 |

K Subt I

UNCLASSIFIED 406 165

SECURITY CLASSIFICATION OF THIS PAGE (When Data Entered)

that stress wave rivet installations offer significant potential weight saving for structures designed to a damage tolerant criteria.

Grumman Research Department Report RE-587

EVALUATION OF DYNAMICALLY RIVETED JOINTS

by

Basil P. Leftheris[+]
H. Eidinoff[*]
and
R.E. Hooson[*]

Final Report on Contract No. N62269-77-C-0478

July 1979

Approved by: Richard A. Scheuing
Richard A. Scheuing
Director of Research

[+] Principal Investigator

[*] Grumman Engineering Department

FOREWORD

This research and engineering program has been conducted by the Fluid Dynamics Directorate of the Grumman Research Department, Grumman Aerospace Corporation, Bethpage, New York, under Contract No. N62269-77-C-0478. Dr. Basil P. Leftheris was Principal Investigator. The contract was administered by the Air Vehicle Technology Department, Naval Air Development Center, Warminster, Pennsylvania, with Paul Kozel providing technical liaison. The report summarizes work performed during the period October 1, 1977 through September 30, 1978.

The test portions of the program were performed by Mr. R. Wigger of the Elements and Materials Test Section under the direction of Mr. D. Layton. Inspection of the specimens was done by the Grumman Quality Control Department. Mr. E.R. Ranalli of the Engineering Structural Analysis section made some valuable contributions to the program.

SUMMARY

The purpose of this program was to evaluate the advantages of dynamically installed rivets in aircraft structures. This was accomplished primarily by testing a large number of three-rivet specimens made of aluminum alloy 2024-T81 material and riveted with the Grumman Stress Wave Riveter (SWR). To establish the suitability of riveting aircraft structures with the SWR in accordance with recent damage tolerance criteria, each hole was precracked using constant amplitude loading. The SWR method of riveting expands the rivet radially at high accelerations that results in plastic deformation of the surrounding material. The process "cold works" the material and leaves compressive residual stresses around the rivet to prevent crack growth under loading.

Precracked specimens riveted with the SWR were fatigue tested under both spectrum and constant amplitude loadings. Spectrum tests were conducted using a reduced F-14 wing fatigue spectrum which included both positive and negative loading cycles. The greater part of the spectrum tests were conducted with a net stress at limit load equal to 35 ksi (241 MPa). Complete arrest of crack growth was evident in all these tests. Such behavior was theoretically predicted by calculating the stress intensity factor K_I. Explicit equations for the residual stresses permitted integration of the K_I equation. It was found that for the precrack sizes of 0.05 - 0.025 in. (1.27 - 1.016 mm), the K_I values were near zero, an indication of no crack growth.

Other tests were carried out at constant amplitude loadings that supplied crack growth characteristics of the specimens riveted with the SWR. Comparison of the results was made with open hole and Hi-lok fastened specimens.

A limited evaluation performed to establish design values for static, fatigue, and damage tolerent (precracked structure) allowable stress levels indicated a significant potential weight saving when allowable stresses for precracked holes were based on SWR-riveted values.

The results obtained from this program indicate that the SWR can arrest cracks consistently, while simultaneously installing a relatively inexpensive rivet. It is recommended that consideration be given to the use of the SWR process in meeting damage tolerance requirements for aircraft structures.

TABLE OF CONTENTS

LIST OF ILLUSTRATIONS

LIST OF ILLUSTRATIONS (contd)

LIST OF TABLES

1. INTRODUCTION AND BACKGROUND

It has been known for some time that riveted joints of aircraft structures are frequently critical points where structural cracking occurs. Various causes were identified over the years that attributed early failures to both the structural design (selection of materials and design allowables) and manufacturing methods. Many causes of structural failure are hidden, that is, not identifiable by established inspection procedures. For example, the buckling of the rivet inside the hole can not be seen from the outside, although it can cause uneven load distribution along the shank of the rivet. Other examples of hidden causes are the ovality of straight holes, and the lack of precision of the taper holes, that could not be controlled adequately through inspection. The viscous sealants used in squeezed riveting methods also create serious problems when trapped hydrostatically between the rivet and hole, and then dry out, leaving voids that cause fuel leakages, stress corrosion and galling.

The use of various types of interference fit fastener systems in aircraft structural applications has been extensive in recent years, and a variety of these fasteners are presently available to the industry. The advantages obtained by the use of such fasteners lies principally in the area of fatigue design. Depending on the type of fastener, the hole is either "propped" or "cold worked" or subjected to a combination of these operations, and as a result, either or both the effective alternating and mean stresses in an applied fatigue loading cycle are reduced, with a subsequent improvement in fatigue life.

In the structural design of aircraft joints, all "interference fasteners" do not possess a common remedy for improving fatigue life, and considerable differences exist among fastening systems that: a) volumetrically fill a hole; b) expand the hole radially, resulting in tension hoop stress and compression radial stress, and c) expand the hole radially until the material yields plastically, but then surround the rivet, through elastic recovery, with compressive residual stresses in both the hoop and radial directions. The most beneficial effects are those of (c). To distinguish these effects from others, the words "cold working" the hole were given to any method that left each hole with residual compressive stresses.

One system that requires nonprecision holes, utilizes inexpensive rivets, and cold works the holes, leaving compressive residual stresses behind it, is the Stress

Wave Riveter (SWR) (see Fig. 1). The capacitor bank at left supplies the electrical energy that is converted to a stress wave in the tool. The black control box sitting on the capacitor bank ensures that each pulse delivered is within specifications for the particular fastener being upset. The rivets in this case are bucked at the tail, the countersunk head being supported by a specially designed bucking bar. The SWR has been used in the Grumman F-14 since 1970, installing straight pins with interference in the wing box beam, and also repairing rivets in the titanium wing structures. It was investigated by the USAF in 1972 (Ref. 1) where in fatigue rating of precracked specimens it was found to possess clear process advantages* over other fastening systems.

The SWR's principle of operation was analyzed both theoretically and experimentally (Ref 2). Explicit equations to calculate the biaxial (radial and hoop) residual stresses were derived (Ref 3) for SWR-installed rivets that can easily provide the necessary information in riveting applications (see Appendix A). The results of a typical case are shown in Figs. 2 through 8 for 2024-T3 aluminum. Analytical results were checked with the Moire' fringe method (see Ref. 4 and Fig. 8). Furthermore, results of fatigue testing of aluminum specimens with radial cracks, riveted with the SWR, showed that cracks of 0.05 in. (1.25 mm) or less, did not grow during spectrum fatigue. Other authors (Ref. 5) have also shown the advantages of cold working the hole, especially the improvement of fatigue life where cracks are present. The SWR method combines: a) the fatigue advantages of cold working the hole, b) the cost advantages in the use of ordinary rivets instead of the more expensive precision fasteners, c) the manufacturing advantages of non-precision holes and "forgiveness" in the shop whenever oval or nonaligned holes pass inspection undetected, and d) the advantage of relaxed inspection procedures.

---

*The SWR-driven rivet expands radially with high velocity, cold working the material around it as it deforms to the shape of the hole. There is no need to cold work the hole and then install a fastener; instead, all the effort is combined in one operation with the SWR.

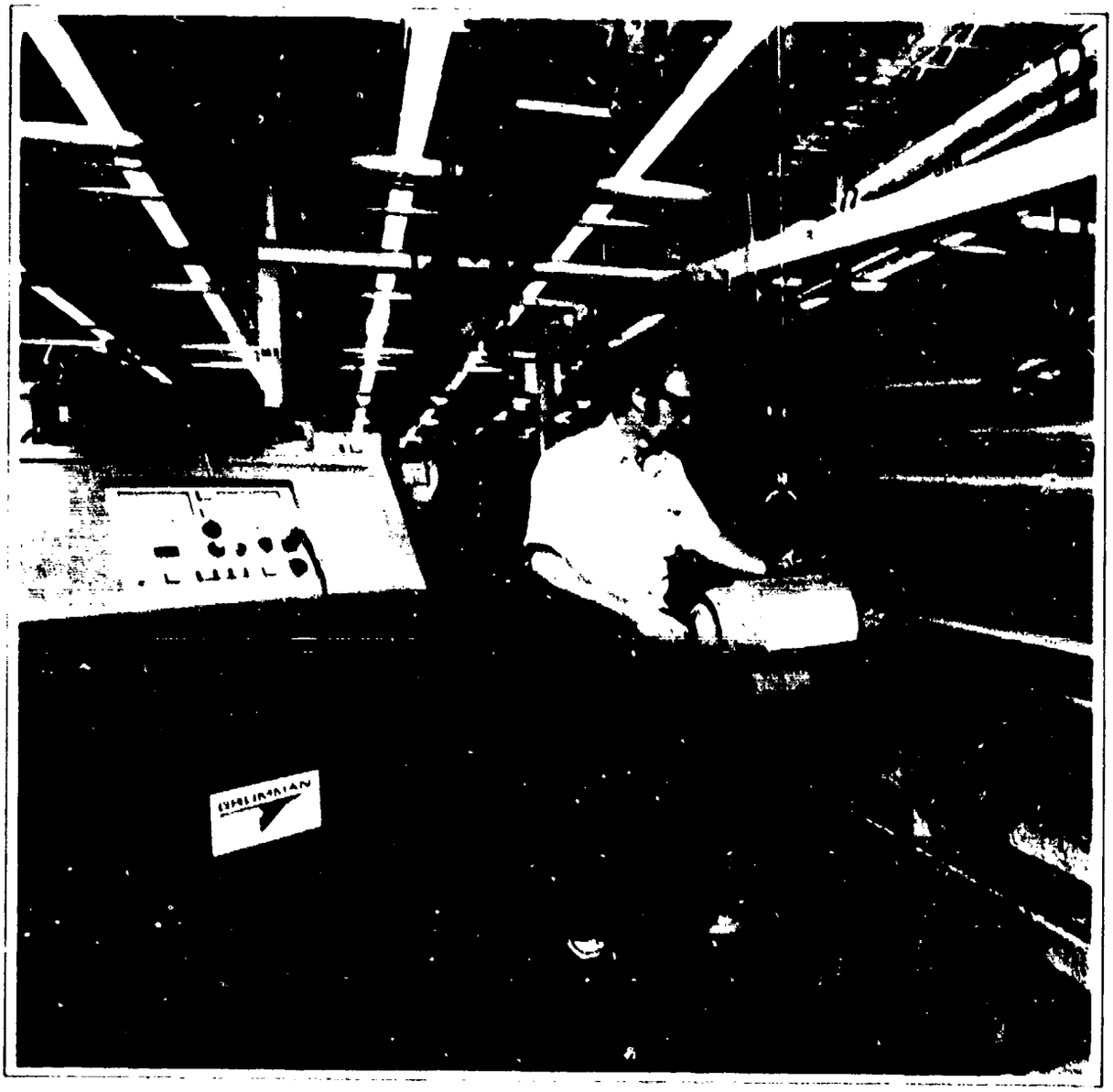

2863 006W

Fig. 1 Stress Wave Riveter Being Used in Production of F-14 Titanium Wing Skins

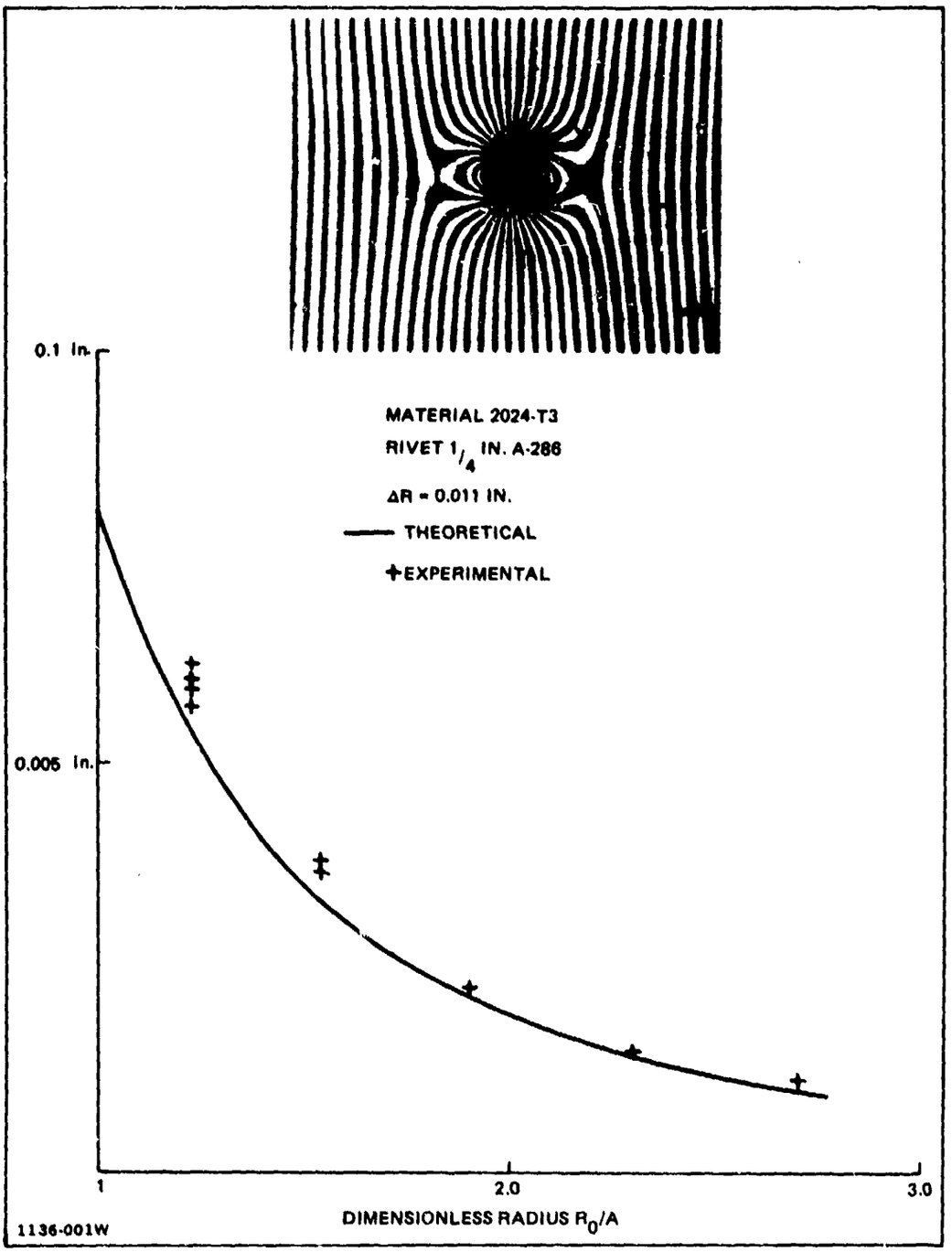

Fig. 2 Residual Hoop Strain vs Radial Distance, ΔR = 0.011 Radial Expansion

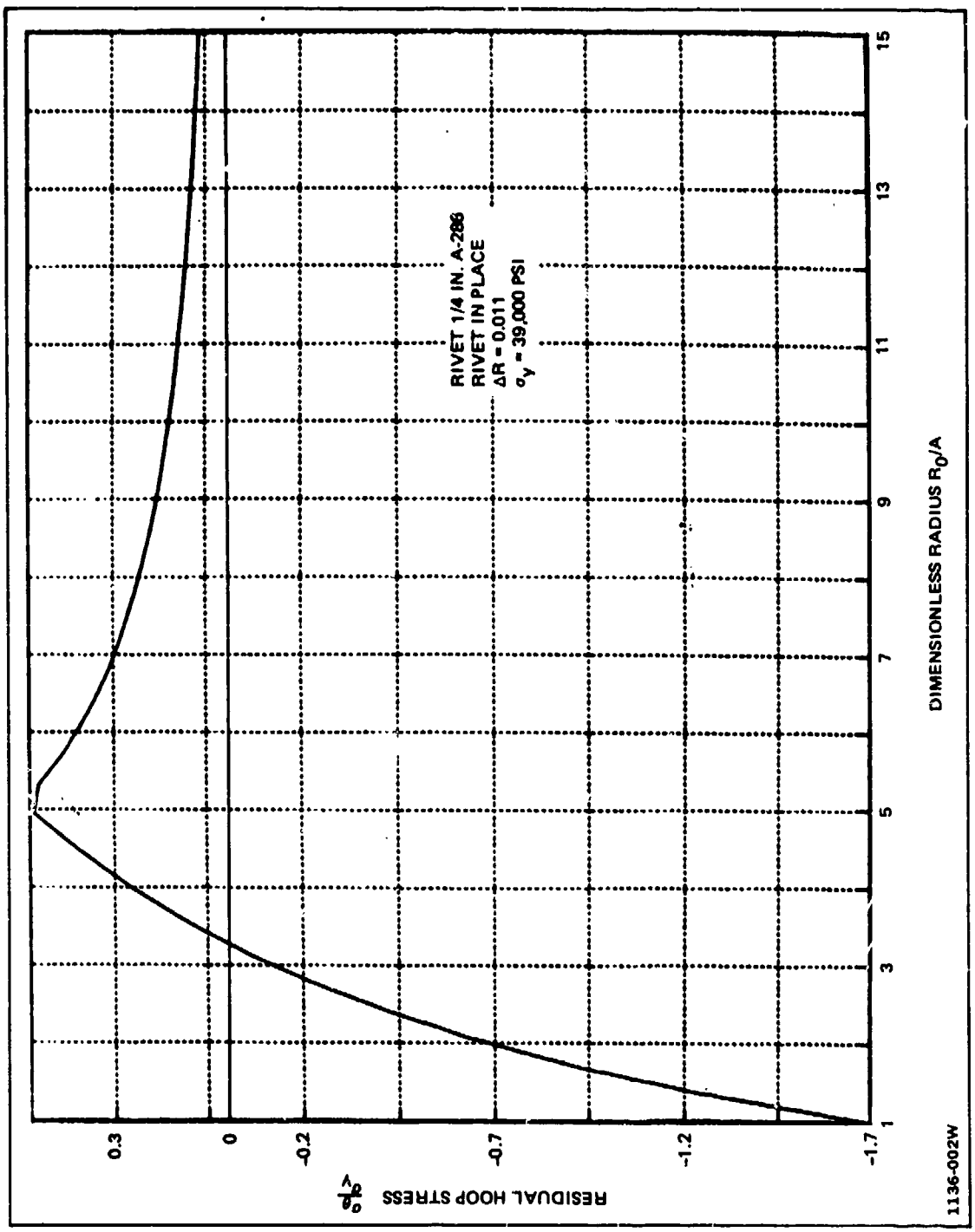

Fig. 3 Residual Hoop Stress vs Radial Distance, AL 2024-T3

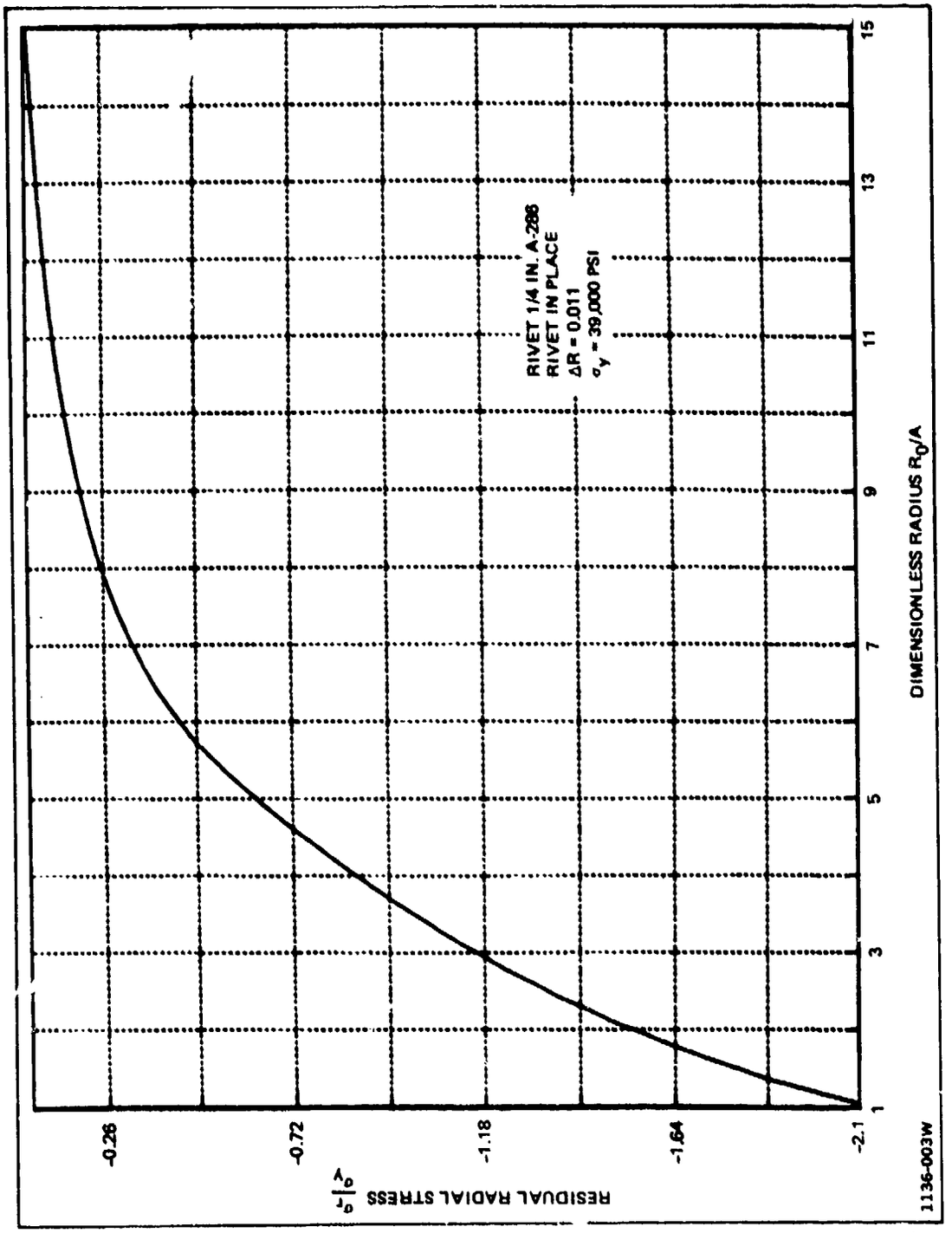

Fig. 4 Residual Radial Stress vs Radial Distance AL 2024-T3

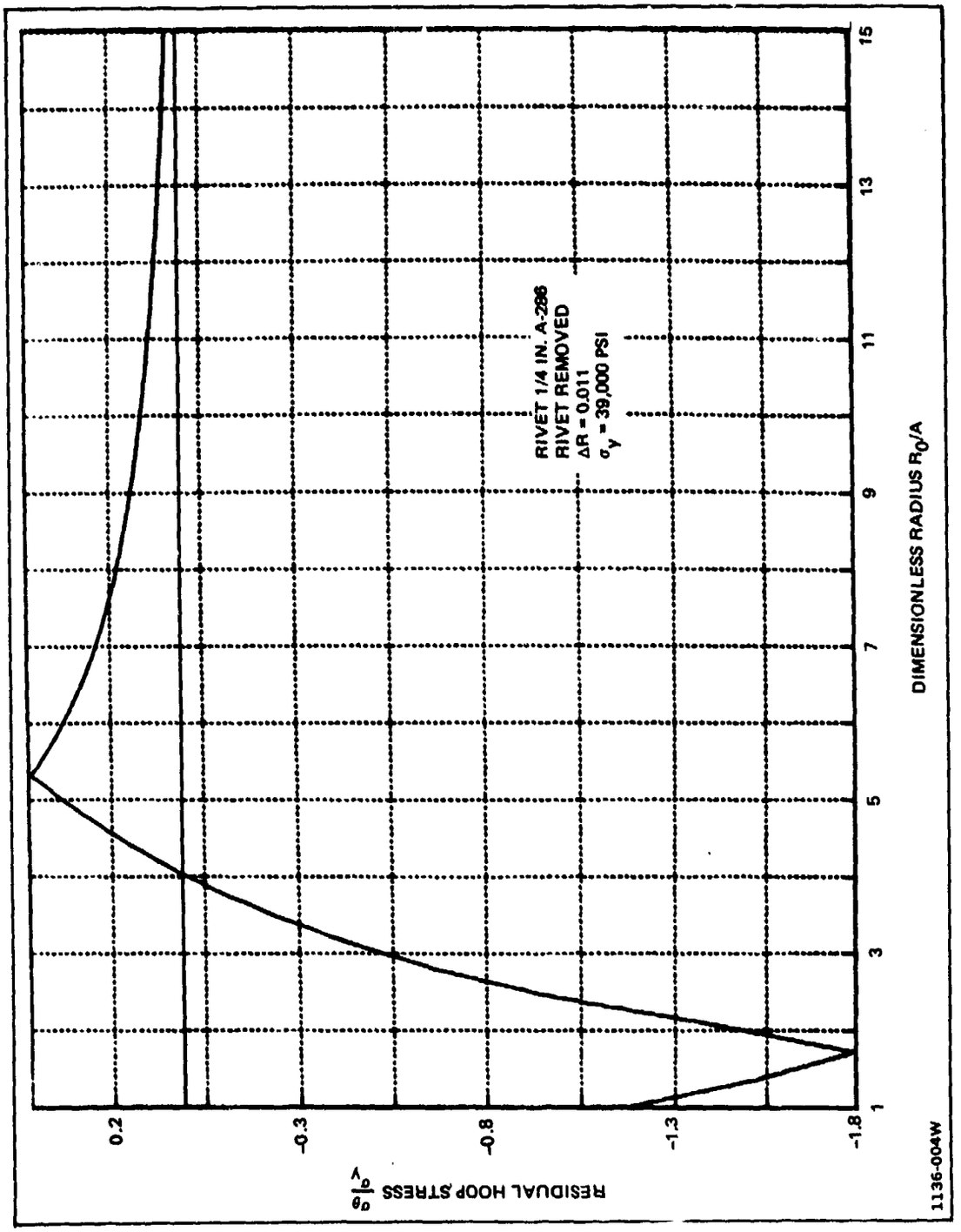

Fig. 5 Residual Hoop Stress vs Radial Distance, AL 2024-T3

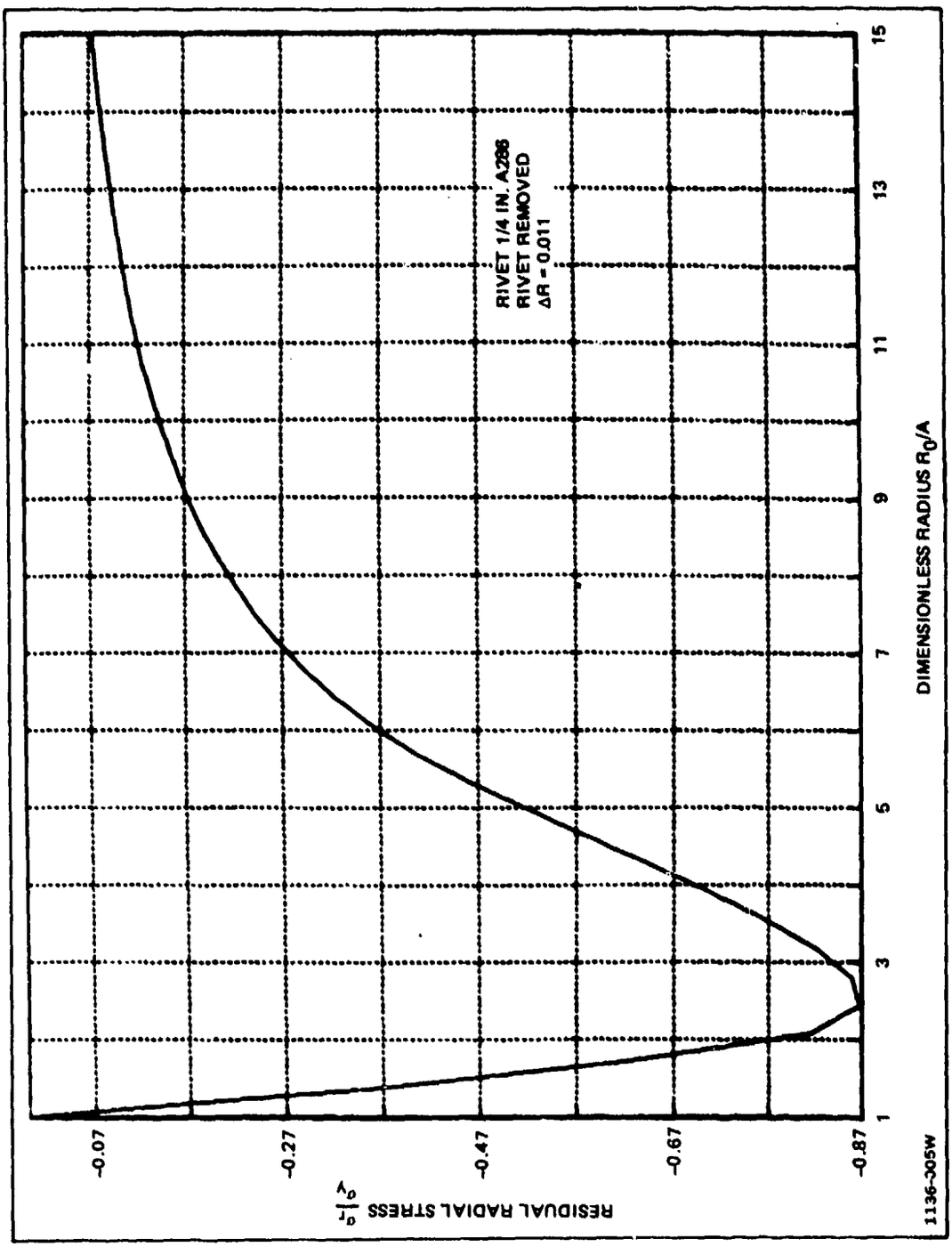

Fig. 6 Residual Radial Stress vs Radial Distance, AL 2024-T3

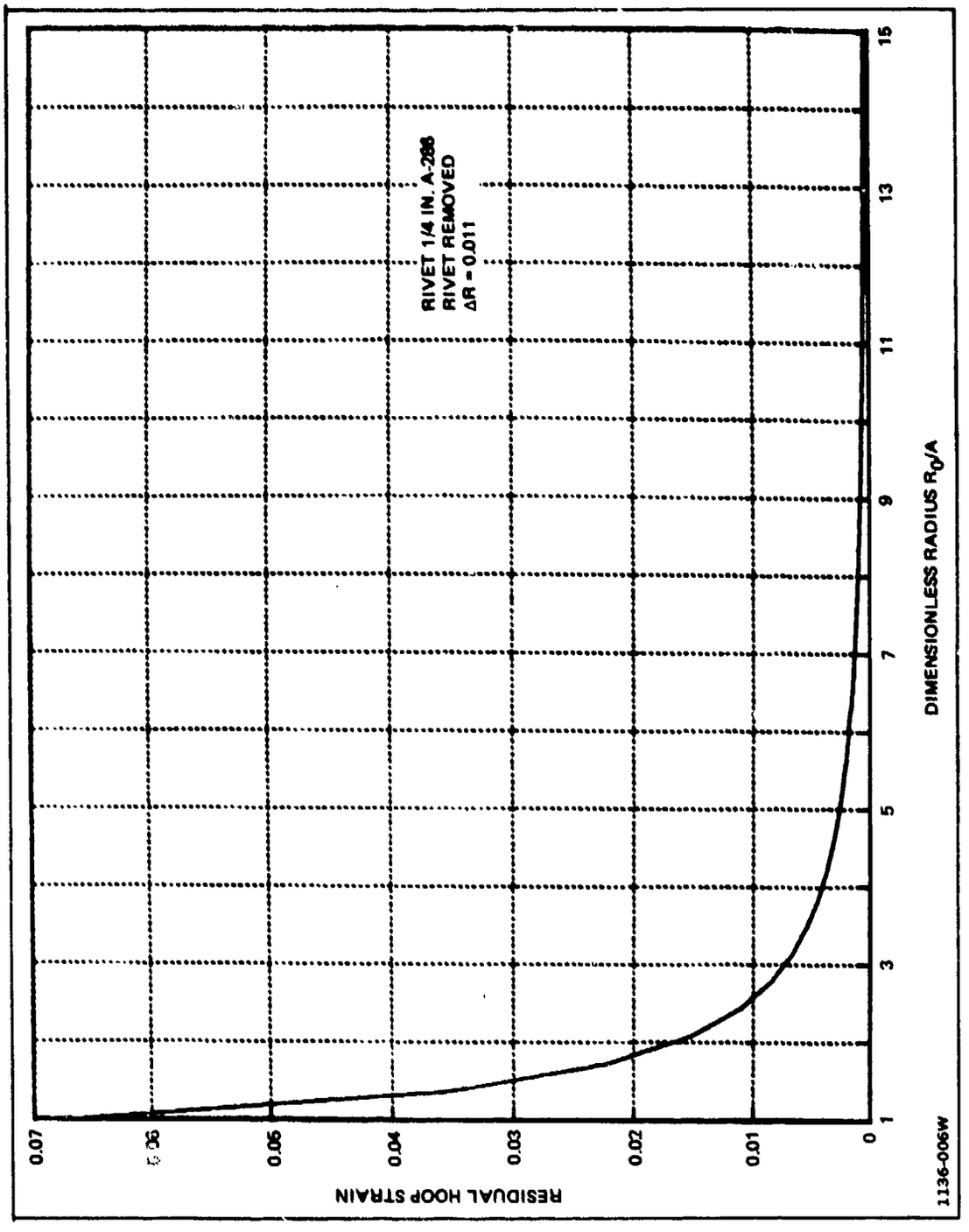

Fig. 7 Residual Hoop Strain vs Radial Distance, AL 2024-T3

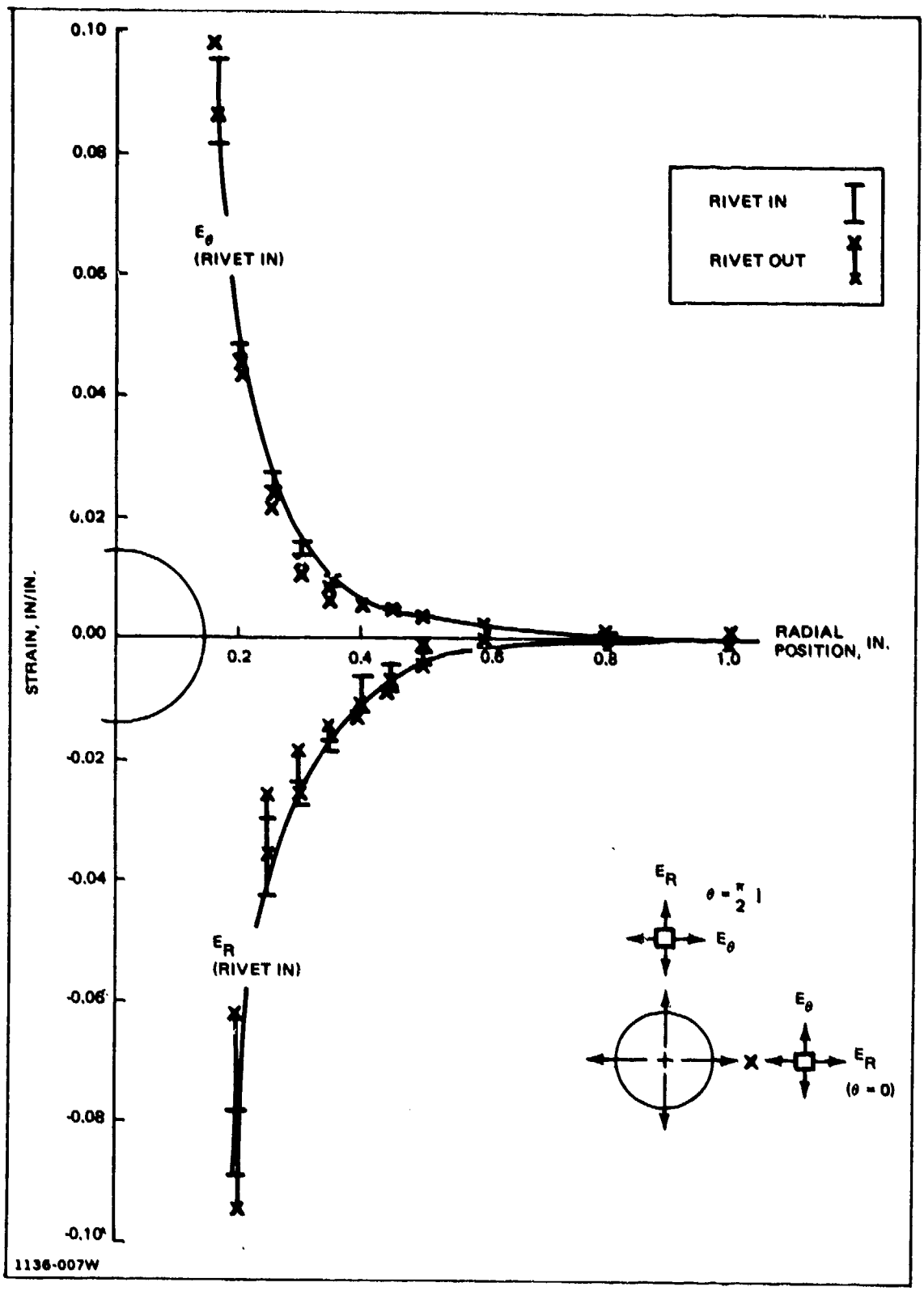

Fig. 8 Residual Principal Strain Distributions, Measured with the Moiré Fringe Technique (Ref. 4), in a Specimen Riveted with the SWR

2. SPECIMEN PREPARATION

All test specimens were prepared from 0.125 in. (3.18 mm) thick sheets of 2024-T81 aluminum alloy, the grain running with the long dimension. The tensile properties of the sheet material were evaluated and the results summarized below.

F_{ty}, psi	59,200 (408.2 MPa)
F_{tu}, psi	66,900 (461.3 MPa)
%e	8.4 (in 2 in.)
%RA	20.8
E, 10^6 psi	10.68 (73.6 MPa)
Rupture Stress, psi	73,300 (505.4 MPa)

Single sheet plain open-hole and 100° countersunk open-hole dog-bone shaped fatigue specimens of the general configuration shown in Fig. 9 were prepared. A number of the plain open-hole specimens were provided with fatigue generated precracks at the test hole edges.

Filled-hole specimens, consisting of two sheets (i.e., a "head" and "tail" sheet) joined together at mid-section with a single fastener, or with multiple fasteners, were prepared. In addition, single sheet filled-hole specimens with back-up washers were also prepared. Specimens of each type were provided with fatigue generated precracks at the fastener hole edges while others were left uncracked. Furthermore, individual two-piece laminated specimens were provided with precracks in either the "head" or the "tail" sheet, or in both sheets.

The specimens containing a single fastener had a constant radius reduced test section as shown in Fig. 10. The multifastened specimens were dog-bone shaped as shown in Fig. 11 and 12.

Two countersunk fastener types were used, the subject GR501W A-286 steel rivets and, to provide baseline data, clearance fit GB510B3-4 steel Hiloks. The A-286 rivets (3/16 in. diameter) were dynamically installed using the Stress Wave Riveter (SWR). A predetermined interference fit of 0.005-0.006 in. (127-152 mm) was used. Final hole preparation in these specimens was such that a sliding fit existed between rivet and hole prior to the riveting operation. The Hilok installations were made in accordance with the Manufacturer's installation procedures.

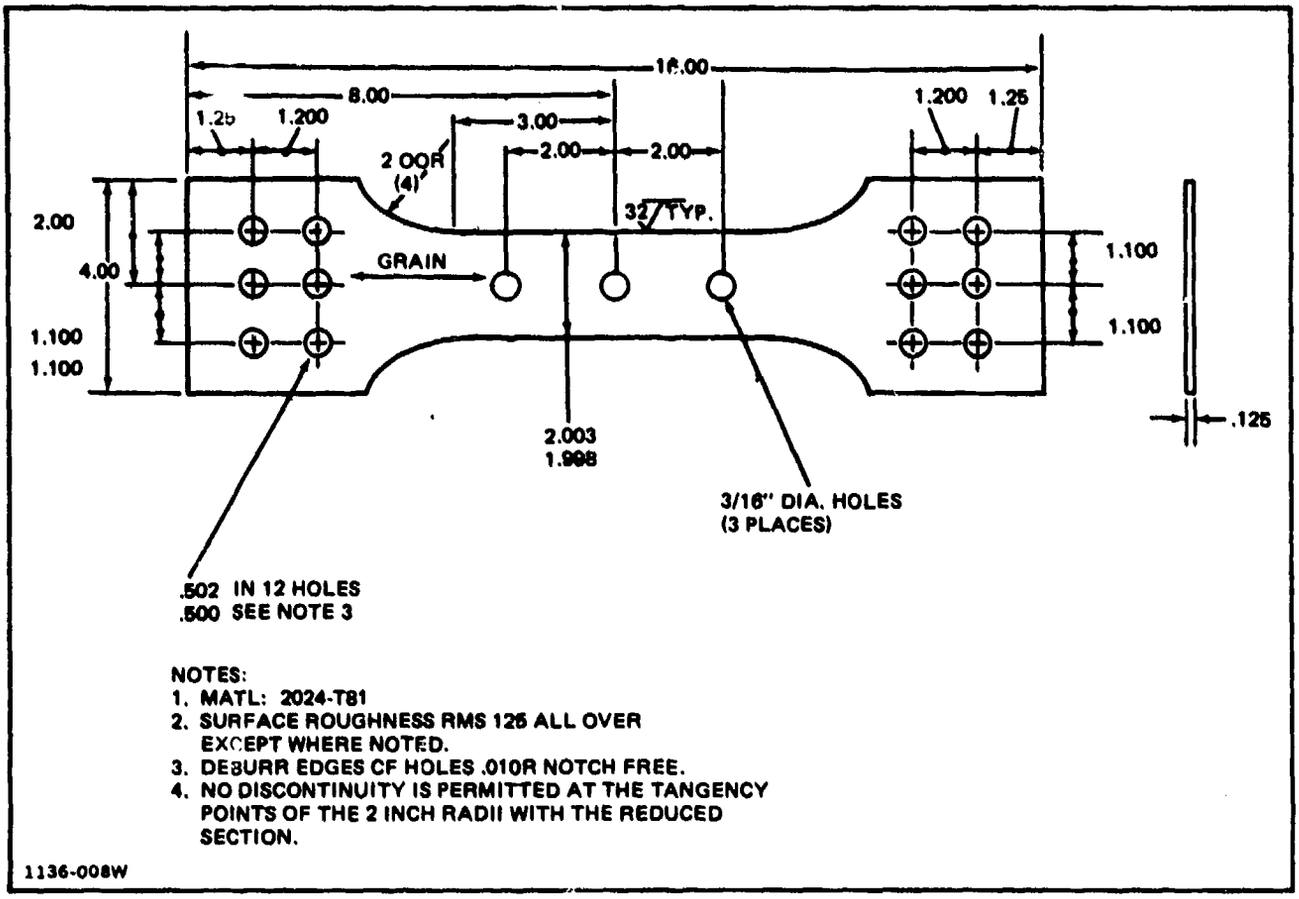

Fig. 9 Open Hole Specimen

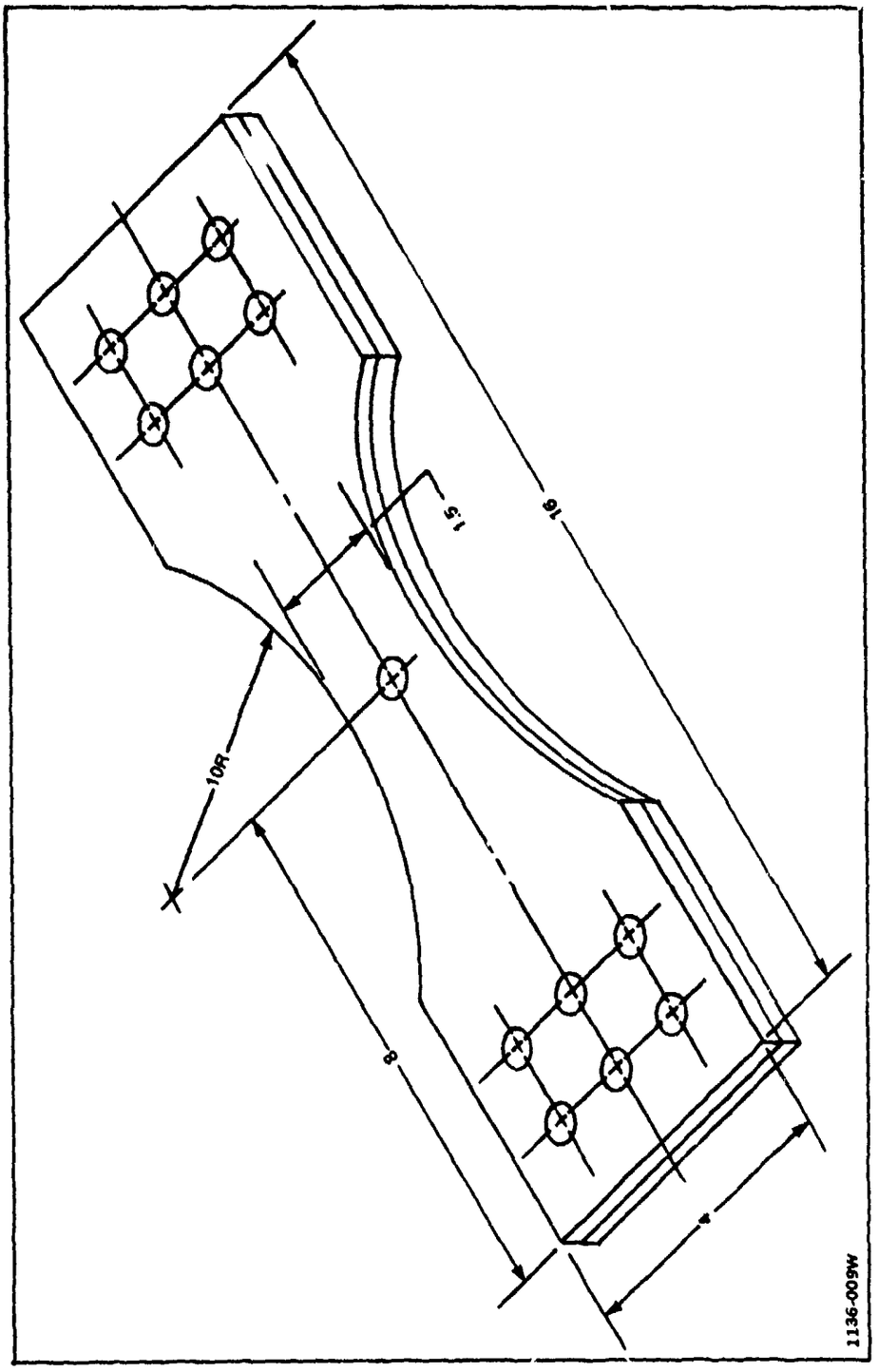

Fig. 10 Two-Piece Specimen with Single Unloaded Fastener

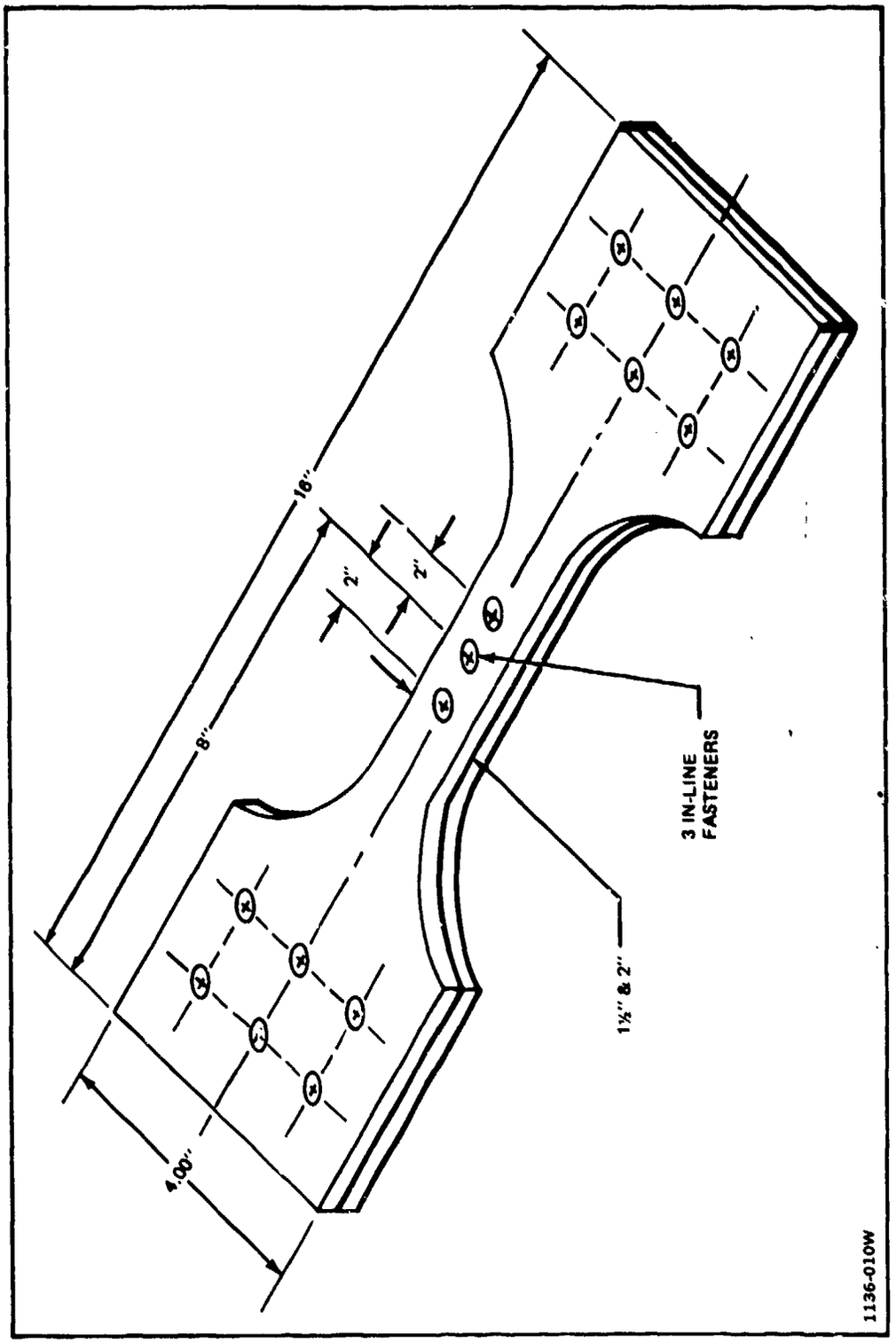

Fig. 11 Two-Piece Specimen with Three Unloaded Fasteners

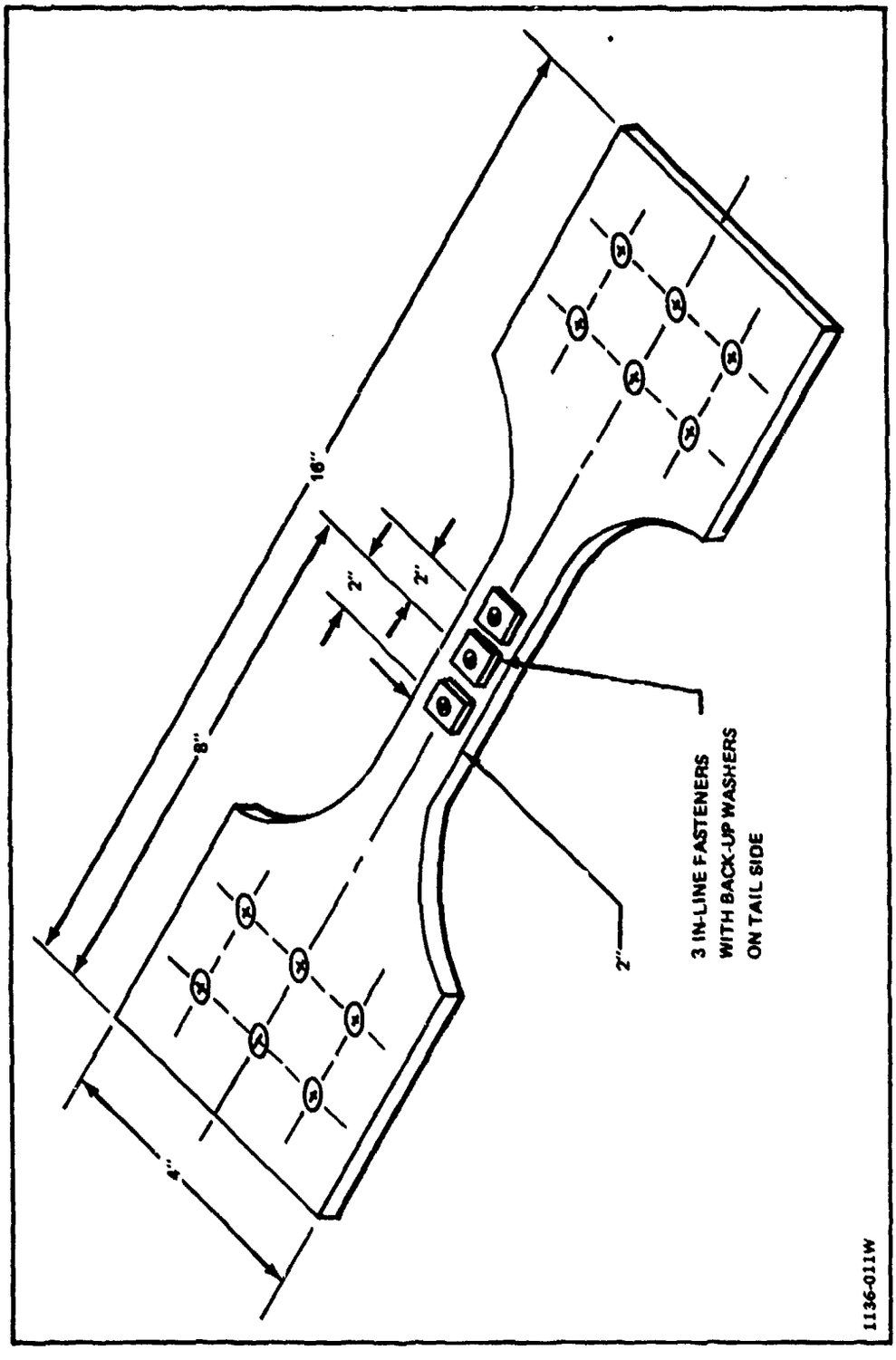

Fig. 12 Single Sheet Specimen with Three Fasteners and Washers

The spectrum fatigue loading was applied using a servo-hydraulic system controlled by a preprogrammed, electronic, load feedback system utilizing a precalibrated load cell and a punched paper tape sequencer. A constant force fatigue machine equipped with a 5:1 load multiplier and automatic preload control unit was used for most of the constant amplitude fatigue work. The servo-hydraulic system described above was also used. The static loading was applied with a universal testing machine equipped with an autographic load-strain recorder and a precalibrated load indicator.

Sheets to be precracked were initially provided with 0.100 in. (2.54 mm) diameter pilot holes located at the positions of final fastener installation. One edge of each pilot hole was notched with a sharp edged tool to facilitate crack initiation. Crack initiation was then accomplished in a direction normal to the load application using an applied cylic net stress of 20 ksi (138 MPa), R = +0.05. The cracks were then extended to the desired length using a net stress of 15 (103 MPa), R = +0.05. The precracked holes were then opened up to a nominal 0.189 in. (4.8 mm) diameter leaving a through-the-thickness crack measuring from 0.025 to 0.040 in. (635-1016 mm) from the hole edge. Extended crack lengths measuring up to 0.080 in. (2.03 mm) from the hole edge were also provided. In most cases, 15,000 cycles at 20 ksi (138 MPa) were required to initiate the cracks at all three hole locations. An additional 30,000 cycles at 15 ksi (103 MPa) were then required to extend the cracks to the desired lengths. For specimens with three precracked holes having one crack growing more rapidly than the others, a clamp was applied to the region of the faster growing crack to retard its crack propagation rate, and thus ensure that all three precracks had nearly uniform lengths.

3. PROGRAM OVERVIEW

Demonstrating the fatigue advantages of joints riveted with the SWR was the purpose of the work performed under this program. We carried out two series of tests: (a) "spectrum fatigue loading", and b) "constant amplitude fatigue loading".

In the first series our aim was to establish a statistical "confidence level" for arresting cracks in specimens riveted with the SWR. For consistency of results we maintained the following parameters constant:

- Material - 2024-T81
- Specimen geometry
- Rivets - 3/16 in. (4.8 mm) diameter made of A286 (Grumman spec GR 501W)
- Radial displacement - (amount of cold work) 0.006 in. (0.152 mm)
- Spectrum loading - F-14 reduced (truncated version of F-14 wing)
- Maximum precrack size range 0.025 - 0.040 in. (0.635 - 1.016 mm)
- Statistical sample size - 15
- Stress at limit load in the spectrum - 35 ksi (241.3 MPa) gross.

Judging from the analytical evaluation of the residual stresses and the stress intensity factor K_I, (calculated from explicit equations derived in Section 5), the cracks were not expected to grow during testing, because the K_I value for cracks 0.025 - 0.04 [illegible] (0.63 - 1.016 mm) was near zero. Indeed, the test results showed that there was no crack growth after 24,000 hours of F-14 simulated flight (the F-14 expected life is 6000 hours). Statistically, therefore, the results present assurance that under the conditions stated the cracks will be arrested.

To establish the extent to which cracks could be arrested, three additional specimens were tested at 45 ksi (310 MPa). They survived without crack growth to 60,000 F-14 simulated hours. In one of the specimens, crack propagation did develop and failure occurred at 67,000 hours.

The complete matrix of specimens tested under the same conditions stated for spectrum fatigue is given in Table 1 below:

TABLE 1 TEST MATRIX: SPECTRUM FATIGUE LOADING

SPECIMEN TYPE/FASTENER	DESCRIPTION	SPECIMEN QUANTITY
CONTROLS (SINGLE SHEET)	A. OPEN-HOLE	2
	B. COUNTERSINK OPEN-HOLE	6
	C. PRECRACKED OPEN-HOLE	7
STRESS WAVE DRIVEN RIVETS (GR501W)	A. TWO-PIECE LAMINATED WITH PRECRACKED HEAD SHEET ONLY	
	(1) 0.25-0.040 CRACK	18
	(2) 0.080 IN. CRACK	5
	B. SINGLE PRECRACKED SHEET WITH WASHERS	3
CLEARANCE FIT GB51083-4 STEEL HILOKS	A. TWO-PIECE LAMINATED WITH PRECRACKED HEAD SHEET ONLY	
	(1) NORMAL CLAMP-UP	6
	(2) NO CLAMP-UP	3
	(3) 0.025 – 0.050 IN. CRACK RANGE	
	B. SINGLE PRECRACKED SHEET WITH WASHERS (NORMAL CLAMP-UP)	3
1136-012W		

Constant amplitude tests were carried out in the second series. Crack propagation rates were observed closely for comparison between precracked specimens riveted with the SWR and precracked specimens riveted with Hi-loks or with open holes. In addition, specimens with a single precracked hole and a single sheet were tested for comparison with the standard three-hole, two-sheet specimens. The test matrix for these tests is presented in Table 2.

Additional specimens were tested with both sheets cracked, or either the rivet head sheet or the rivet tail sheet cracked, to find any effects in fatigue life attributable to the geometry of the specimens. None was found. Finally, tests were carried out with a three-hole single-sheet configuration, with a washer attached to each hole and riveted with the SWR to eliminate the carry through load of the second sheet during loading, while maintaining the local effects of the second sheet. An engineering analysis of the crack propagation results is given in Section 6. The K_I values are estimated from the constant amplitude load fatigue curves and compared with the K_I values derived theoretically in Section 5. Furthermore, a simulated F-14 lower wing cover is analyzed with damaged tolerance criteria. The results are tabulated (Table 6) showing the weight penalties with several fastener methods, including the SWR method evaluated in this program. In Section 7, the results of the program are summarized and briefly discussed.

TABLE 2 TEST MATRIX: CONSTANT AMPLITUDE FATIGUE LOADING

SPECIMEN TYPE	DESCRIPTION	SPECIMEN QUANTITY
CONTROLS (SINGLE SHEET)	A. PRECRACKED OPEN-HOLE	3
STRESS WAVE DRIVEN RIVETS (GR501W)	A. TWO-PIECE LAMINATED (SINGLE FASTENER)	
	(1) NO PRECRACK IN EITHER SHEET	3
	(2) PRECRACKED "HEAD" SHEET ONLY	3
	(3) PRECRACKED IN BOTH SHEETS	3
	B. TWO-PIECE LAMINATED (MULTIPLE-FASTENER)	
	(1) PRECRACKED "HEAD" SHEET ONLY	3
	(2) PRECRACKED "TAIL" SHEET ONLY	3
	C. SINGLE PRECRACKED SHEET WITH WASHERS (MULTIPLE FASTENERS)	4
CLEARANCE FIT GB510B3-4 STEEL HILOKS 1136-023W	A. TWO-PIECE LAMINATED WITH PRECRACKED "HEAD" SHEET ONLY (MULTIPLE FASTENERS)	3

4. FATIGUE TESTING

SPECIMEN TESTING

Specimens were examined prior to testing to establish hole surface finish and pre-crack length but standard inspection techniques were generally found to be unsatisfactory due to the small size of the hole.

The initial crack length was therefore measured visually with the specimen under load, prior to the rivet installation. A sampling of specimens was also subjected to post-failure metallurgical examination to establish initial crack lengths. After testing, a sawcut was made along the crack axis from left to right, up to the end of the vertical tool marks. The specimen was then pulled to failure in a tensile test unit, failing at the zone of random fine structure in the center of the picture. The vertical band at the edge of the hole is the crack placed in the specimen before fatigue testing. An example is provided by Fig. 13 which shows a sectional view of a pre-cracked specimen broken statically after spectrum fatigue testing for 24000 equivalent flight hours without failure. The initial crack length was 0.04 in. (1.01 mm) in this case.

Figure 14 shows a pre-cracked specimen that was tested to failure in spectrum fatigue. This specimen failed at 26000 equivalent flight hours at a net limit load stress of 40 ksi, with a pre-crack length of 0.07 in. (1.77 mm). Subsequent crack growth from the initial pre-crack shown in Fig. 14 is typical of these test specimens.

Figures 15 and 16 show the test setup and visual crack growth monitoring using a telescope. Specimens were prevented from buckling by the use of a stabilization frame. All tests were conducted in a laboratory air environment.

STRESS WAVE RIVETING

The SWR-driven rivets were of F-14 production quality. Drilling and riveting was done under accepted Grumman manufacturing procedures.*

*Manufacturing Technology MEPS 15000-066

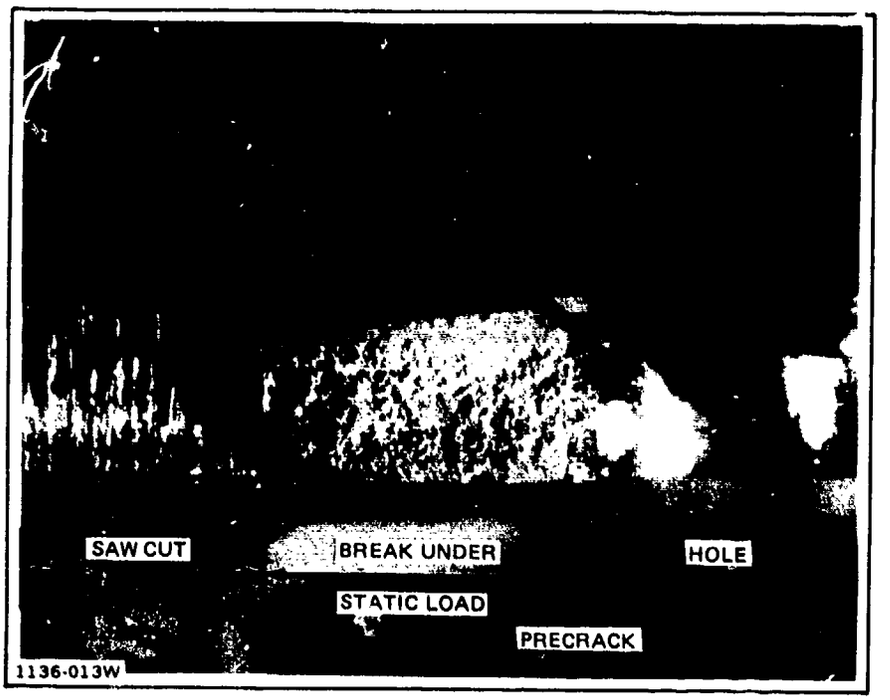

Fig. 13 Section View of Precracked Specimen [0.040 In. (1.01 mm) Crack] with No Subsequent Growth

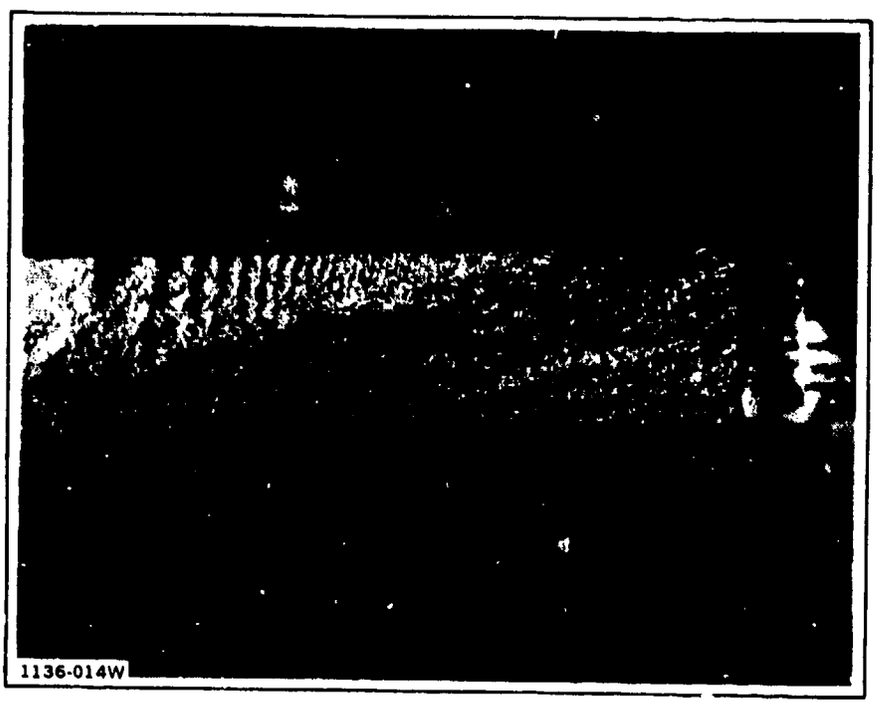

Fig. 14 Section View of Precracked Specimen [0.070 In. (1.77 mm) Crack] with Subsequent Growth

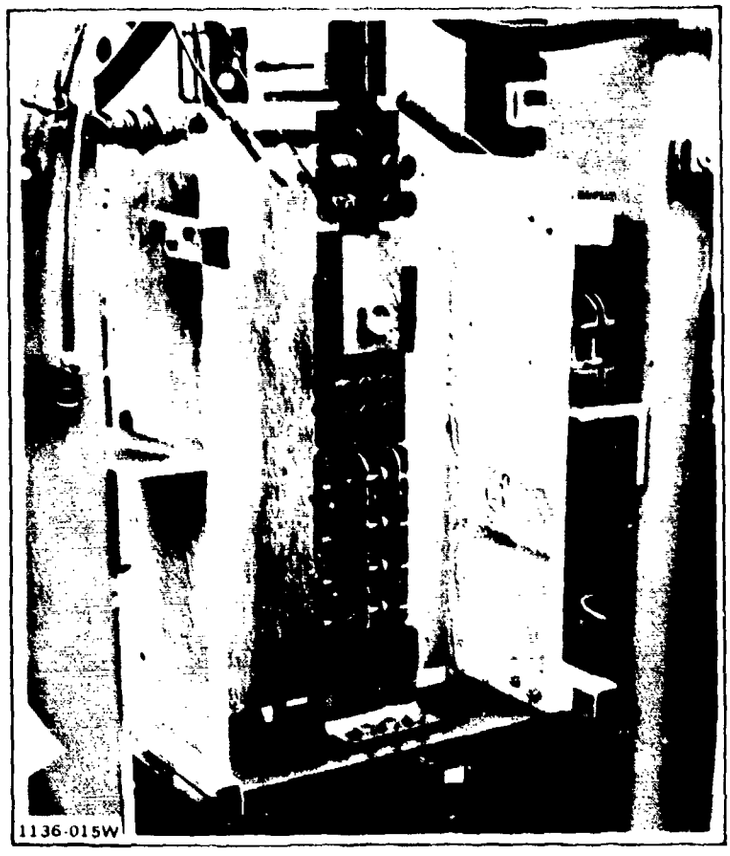

Fig. 15 Test Setup with Parallel Beams to Prevent Bending During Compression Load Cycling

Fig. 16 Telescope Observation of Crack Growth During Testing

Rivet installation with the SWR was performed using the latest manufacturing standards. The holes were drilled with a tolerance of 0.0015 in. (0.0381 mm). Such tolerances are accepted routinely in aircraft manufacturing at Grumman, since drilling is accomplished with automated machines. The rivets were first installed with a snug fit, prior to riveting. Then they were upset using the SWR (SWR setting of 7.5 kv which produces 0.006 in. (0.152 mm) radial displacement). In practice, this procedure prevents gaps under the prefabricated head and provides more uniform cold working of the hole. Furthermore, a slightly domed rivet-set was used in the bucking bar side to expand the prefabricated rivet head. This technique is especially beneficial with GR501W rivets which are made with a slightly domed head. A flat set was used in the SWR tool side (rivet tail).

The SWR method of riveting is capable of accepting considerable variation in hole tolerances ("forgiveness") as was discussed earlier. In this program, however, the purpose was to establish its capabilities under existing manufacturing procedures.

5. DESCRIPTION OF K_I CALCULATION METHOD

INTRODUCTION

Whenever a crack appears in a stress field, there is a redistribution of stress near the crack tip that permits the transmission of the remotely applied force through the tip region (Ref 6). The remotely applied forces affect only the intensity of the stresses near the tip, but not their distribution. The stress intensity factor K_I, therefore, represents the amplitude, or coefficient, of the equation of the stress distribution near the crack tip. The stress intensity factor can also be seen as a limiting case of the stress concentration factor, K_t, for an elliptical hole.

The need to know the stress intensity factor (K_I) in predicting the fatigue life of structural components is well known. With the extensive use of residual stresses in riveted joints, new methods are required to calculate the stress intensity factors which relate the crack length, remote loading, local loading, and structural geometry.

Grandt (Ref 7) and Impellizzeri (Ref 8) used the method of linear superposition to relate local and remote loadings. Both used a weight function similar to the one developed by Bueckner (Ref 9) for evaluation of the integral that gives the values of K_I. In addition, both used a series expansion to relate the edge crack equation to a single crack emanating radially from a rivet hole. Finally, both used numerical integration to evaluate the K_I integral.

In the evaluation of stress intensity factors of holes with cracks, and residual stresses due to SWR-driven rivets, we used the Bueckner function, the explicit equations for residual hoop stress distribution given in Appendix A, and a functions ϕ_1 suggested by Impellizzeri, which corrects for the hole and edge distance geometry in each application.

STRESS INTENSITY EQUATIONS

The stress intensity factor in a hole riveted with the SWR and loaded at infinity can be found through the principle of superposition.

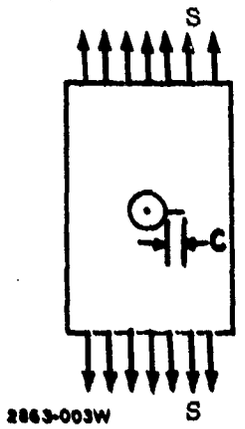

2863-003W

$$K_I = K_{\text{residual stress}} + K_{\text{load}} \tag{1}$$

K_{load} is given by the equation

$$K_{load} = S\sqrt{\pi c}\ \beta_{Bowie} \tag{2}$$

where, $\beta_{Bowie} = \left[\frac{0.8733}{0.3245 + \frac{c}{R}} + 0.6762\right]$

where "c" is the crack length and "R" is the hole radius. The stress intensity factor (K_I) was derived analytically by integrating the following equation:

$$K_{\text{residual stress}} = \phi_1 \cdot \phi_2 \sqrt{\frac{\pi}{2}} \int_0^a \sigma(x)M(x)dx \tag{3}$$

where residual stresses (Ref. 8)

$$\sigma(x) = \alpha + \beta \ln \frac{R_0}{R} + \frac{\gamma}{R_0^2} \tag{4}$$

and

$$M(x) = \frac{1}{\sqrt{c - x}} + \frac{0.6147}{c}(c - x)^{1/2} + \frac{0.2502}{c^2}(c - x)^{3/2}, \tag{5}$$

a weight function suggested by Bueckner. (Ref. 9) The geometry of the crack and the hole are shown below

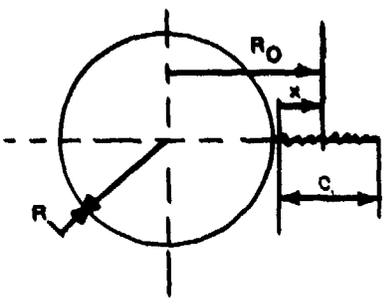

2863-004W

where R_o = a general position in the stress field

The various parameters are

$$\alpha = \frac{2\sigma_y}{\sqrt{3}}\left(1 + \ln\frac{R}{R'}\right) - \frac{E}{(1+\mu)} \cdot \frac{R}{(R')^2} \cdot F + (\Delta P)\left(\frac{R}{b}\right)^2 \tag{6}$$

$$\beta = \frac{2\sigma_y}{\sqrt{3}} \tag{7}$$

and

$$\gamma = (\Delta P)R^2 \tag{8}$$

where

$$R' = \sqrt{\frac{E}{(1+\mu)} \cdot \left(\frac{R}{\frac{\sigma_y}{\sqrt{3}}}\right) \cdot F} \tag{9}$$

F = radial displacement (amount of cold work)

σ_y = yield stress of the material

E = Young's modulus

μ = Poisson's ratio

b = edge distance or 10R, whichever is least

$$(\Delta P) = \left\{\frac{2\sigma_y}{\sqrt{3}} \ln\frac{R}{R'} - \frac{E}{1+\mu}\frac{R}{(R')^2} F\right\} \left\{1 - \frac{\left(\frac{1+\mu_1}{1+\mu_2}\frac{E_2}{E_1}\right)}{1 + \left(\frac{1+\mu_1}{1+\mu_2}\right)\frac{E_2}{E_1}}\right\} \tag{10}$$

where the subscript 1 refers to the material around the rivet and subscript 2 refers to the rivet material.

$$\phi_1 = 1 - 0.6449\left(\frac{c}{R}\right) + 0.8964\left(\frac{c}{R}\right)^2 - 0.7327\left(\frac{c}{R}\right)^3 + 0.3335\left(\frac{c}{R}\right)^4 \tag{11}$$

ϕ_2 is a correction factor for the effect of finite width.

Integration of Eq (3) results in

$$K_{\text{residual stress}} = \phi_1 \sqrt{\frac{\pi}{2}} \left\{ 2.5\alpha \sqrt{c} + \beta \left[\frac{4a}{3R} - \frac{16}{30}\left(\frac{c}{R}\right)^2 + 0.6147\left(\frac{4c}{15R} + \frac{16}{105}\left(\frac{c}{R}\right)^2\right)\right]\sqrt{c} + \gamma \left[\left(\frac{c}{R} - 3 + \frac{1}{R} + R\sqrt{\frac{1}{c+R}}\right)\sqrt{c} + \left(\frac{2(c+R)}{\sqrt{c+R}} + \frac{1}{\sqrt{c+R}} + \frac{1}{(c+R)\sqrt{c+R}}\right)\tanh^{-1}\sqrt{\frac{c}{c+R}}\right]\right\} \quad (12)$$

Restrictions: The maximum crack size that the above equations can be used with is $\frac{c}{R} < 1$. For $\frac{c}{R} > 1$, there is an error due to the divergence of a logarithmic series introduced in the integration.

K_I CALCULATIONS

The compressive residual stress distributions for 0.006 in. (0.152 mm) radial displacement were calculated for 3/16 in. (4.82 mm) holes and 2024-T81 material. The results are given in Figs. 17, 18 and 19. The dimensionless radius is the ratio of $(R_0/R) = \frac{\text{radial distance}}{\text{hole radius}}$. The significance in the plots is that the biaxial compressive field (cold work) extends up to $R_0/R = 2.4$ (see Fig. 19). This is dependent on the radial displacement which, in this program, was maintained constant at 0.006 in. (0.152 mm).*

The K_I's were calculated from Eqs. (2) and (12) using a computer. The results are shown in Figs. 20, 21 and 22. In each figure there are two plot lines: the upper graph corresponds to the K_I without residual stresses, and the lower corresponds to the K_I with residual stresses. Considerable reduction in the K_I value of the residual stress case is shown in Figs. 20 and 21.

---

*In this program the radial displacement was chosen first before the fatigue evaluation of the specimens. In design analysis the fatigue requirements will determine the radial displacement. Further discussion on this approach is given in Section 6.

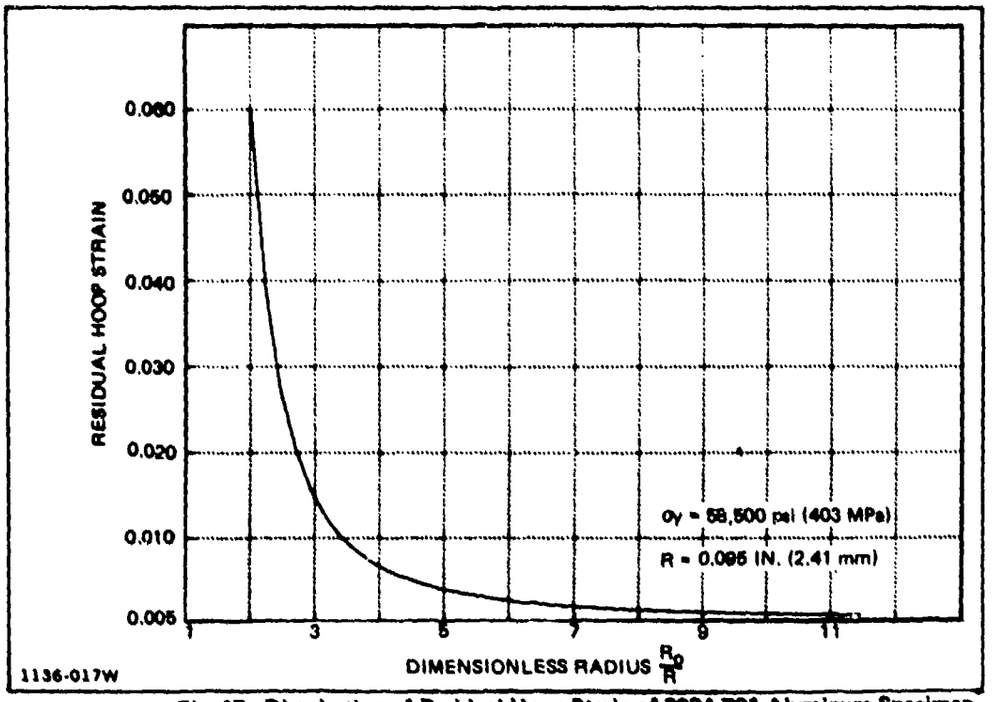

Fig. 17 Distribution of Residual Hoop Strain of 2024-T81 Aluminum Specimen SWR Riveted with 3/16 In. (4.83 mm) Diameter A-286 Rivet with 0.006 In. (0.152 mm) Radial Displacement

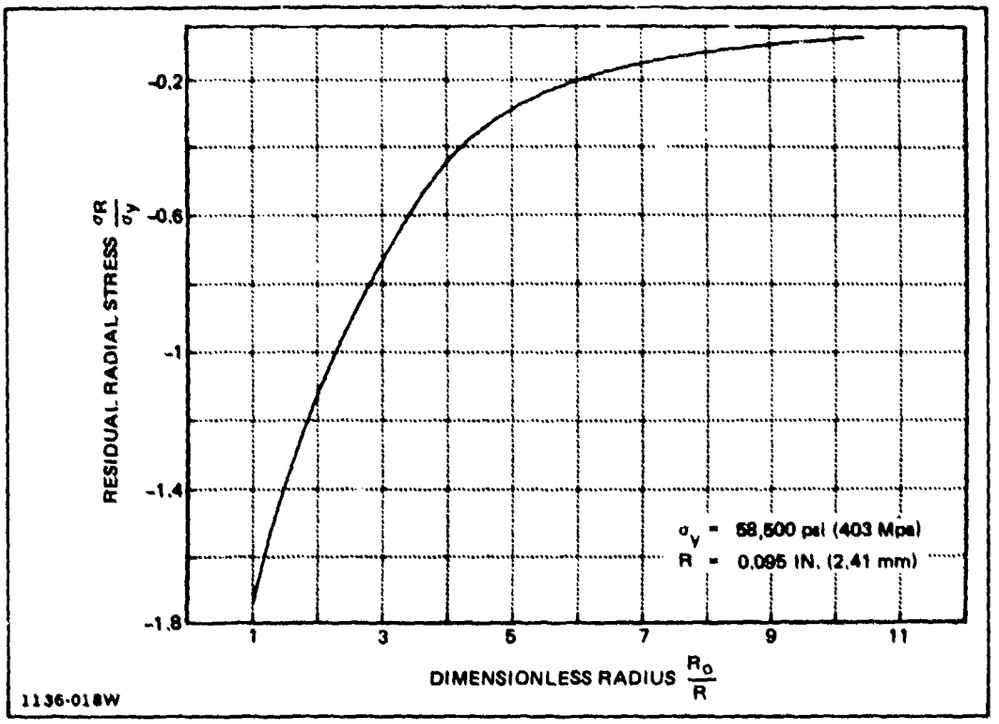

Fig. 18 Distribution of Residual Radial Stress of 2024-T81 Aluminum Specimen SWR Riveted with 3/16 In. (4.83 mm) Diameter A-286 Rivet with 0.006 In. (0.152 mm) Radial Displacement

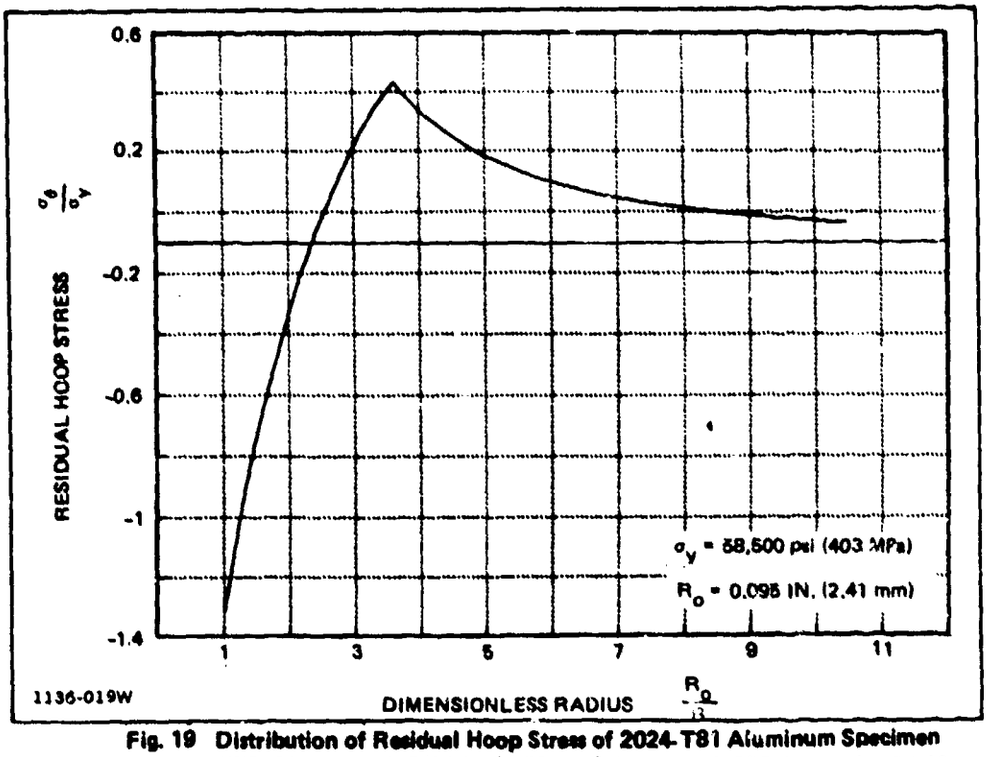

Fig. 19 Distribution of Residual Hoop Stress of 2024-T81 Aluminum Specimen SWR Riveted with 3/16 In. (4.83 mm) Diameter A-286 Rivet with 0.006 In. (0.152 mm) Radial Displacement

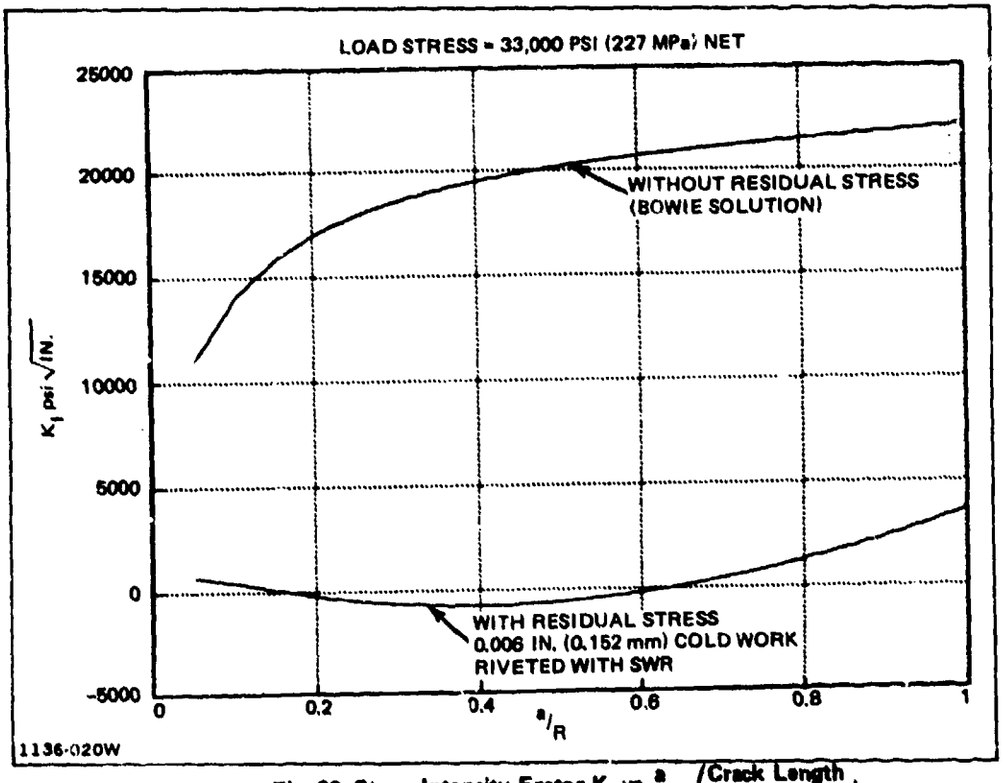

Fig. 20 Stress Intensity Factor K_I vs $\frac{a}{R}$ $\left(\frac{\text{Crack Length}}{\text{Hole Radius}}\right)$

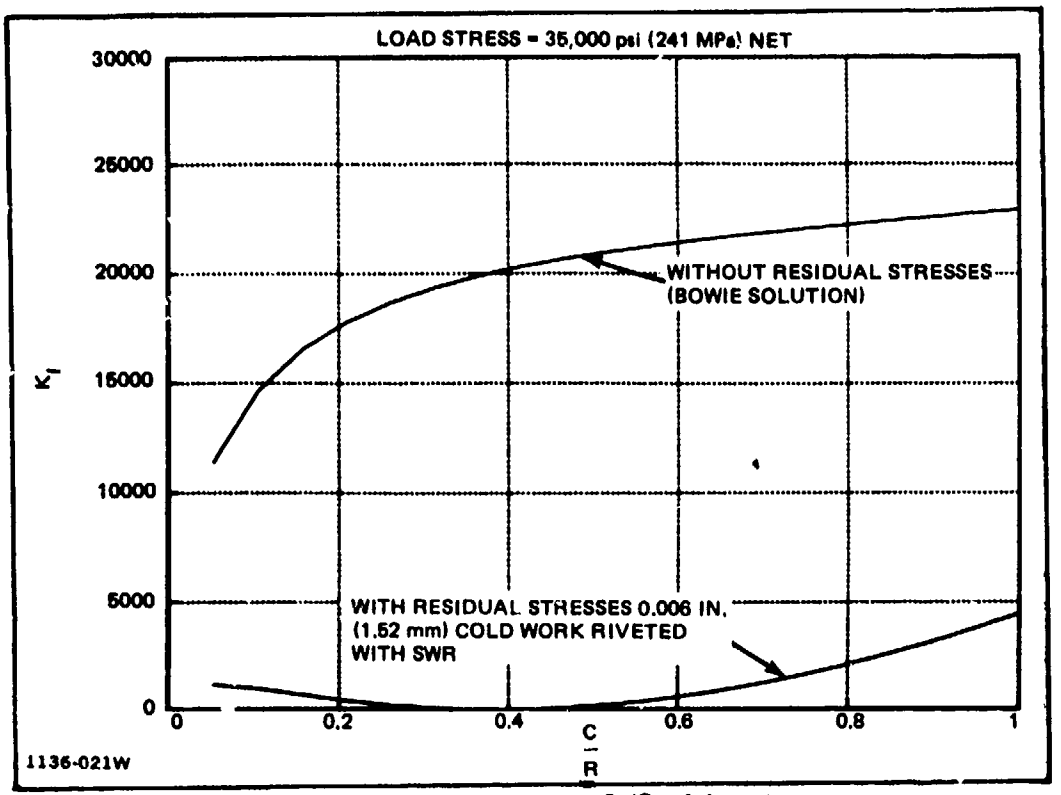

Fig. 21 Stress Intensity Factor K_I vs $\frac{C}{R}\left(\frac{\text{Crack Length}}{\text{Hole Radius}}\right)$

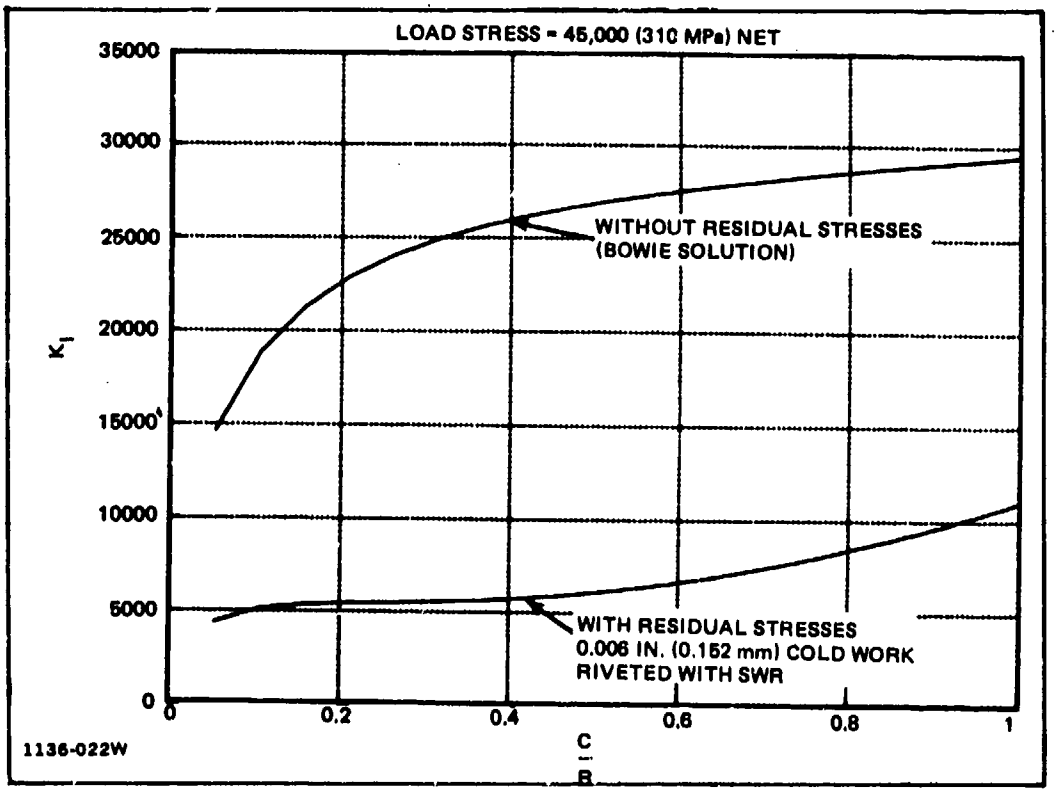

Fig. 22 Stress Intensity Factor K_I vs $\frac{C}{R}\left(\frac{\text{Crack Length}}{\text{Hole Radius}}\right)$

6. FATIGUE CRACK PROPAGATION

CONSTANT AMPLITUDE TESTS

A group of twenty-five specimens were subjected to constant amplitude fatigue loading, in order to obtain some basic data on the growth of cracks at holes containing rivets driven with the Stress Wave Riveter (SWR). All of these specimens were made of 2024-T81 aluminum sheet, having a test section 1.50 in. (38.1 mm) wide, 1/8 in. (3.18 mm) thick, with central 3/16 in. (4.83 mm) fastener holes. Some specimens had single fastener holes in the test section (see Fig. 10), and others had three in-line fastener holes in the test section (see Fig. 11). Four of the specimens were tested without initial cracks, with the remainder having through-the-thickness radial precracks at each fastener hole. The initial crack lengths ranged from 0.020 in. (0.51 mm) to 0.040 in. (1.02 mm). All of the tests were run at a maximum gross stress of 30.6 ksi (211 MPa), and a stress ratio (R) of +0.05 in a laboratory air environment. The results of all the constant amplitude fatigue tests are summarized in Table 3.

A control group of three specimens having precracked open holes were tested and found to have an average life of 3130 cycles. Next, fifteen specimens having precracked holes containing SWR-driven rivets were tested, and the fatigue crack propagation life increased to values ranging from 77,000 to 200,000 cycles, a factor of between 25 and 65. The average increase in life for all the precracked SWR specimens is a factor of 45.

Most of the test articles containing SWR-driven rivets consisted of two 1/8 in. (3.18 mm) sheets fastened together. There was no significant difference in life between specimens having single fasteners in the test section and those having three in-line fasteners. Specimens were tested in the following three categories: precracks in head sheet only; precracks in the tail sheet only; and precracks in both head and tail sheets. No significant difference in life was observed between these configurations. The SWR installation method effectively retards crack growth in both the head and tail sheets. However, when both sheets were precracked, failure always occurred in the head sheet.

TABLE 3 SUMMARY OF CONSTANT AMPLITUDE FATIGUE DATA 3/16 IN. DIA FASTENER HOLES IN 2024-T81 SHEET

Type Specimen	Specimen No.	Post Test Fastener Dia. (in.) Head Sheet	Post Test Fastener Dia. (in.) Tail Sheet	Initial Crack Length - c (in.)	Max. Net Stress (ksi)	Max. Gross Stress (ksi)	Cycles to Failure	Comments
Open Hole Single Sheet Precracks 3 Holes In-Line (Fig. 9)	P2-17			0.025 0.030 0.030	35.20	30.74	3000	Significant growth at all three holes. Failure at bottom hole.
	P2-22			0.040 0.035 0.040	35.10	30.65	3100	Significant growth at all three holes. Failure at middle hole.
	P2-23			0.030 0.025 0.025	35.00	30.57	3300	Significant growth at all three holes. Failure at top hole.
						Average =	3130	
SWR 2 Sheets No Precracks Single Fastener (Fig. 10)	AV-2			0	35.00	30.57	296,000	All crack growth occurred in "head" sheet.
	A-1	0.202	0.206	0	34.80	30.39	260,000	
	A-3	0.206	0.206	0	34.90	30.48	169,000	Failed via initiation at location other than at test hole.
	A-2	0.206	0.206	0	35.00	30.57	149,000	
						Average =	223,500	
SWR 2 Sheets Precracked Head Sheet Only Single Fastener (Fig. 10)	AK-1	0.201	0.204	0.030	35.00	30.57	199,000	Failed via initiation at location other than at precracked test hole. No significant crack growth in head sheet.
	AK-2	0.201	0.203	0.040	35.00	30.57	121,000	
	AK-3	0.200	0.203	0.025	35.00	30.57	138,000	All crack growth occurred in "precracked" head sheet.
						Average =	152,670	
SWR 2 Sheets Both Sheets Precracked Single Fastener (Fig. 10)	AKK-4	0.200	0.202	0.040	34.90	30.48	103,500	All crack growth occurred in "head sheet" only. No significant growth in "tail sheet".
	AKK-6	0.200	0.203	0.015	34.90	30.48	156,200	
	AKK-5	0.201	0.204	0.040	35.00	30.57	194,000	Failed via initiation at site other than precrack. No significant growth of either crack.
						Average =	151,230	
SWR 2 Sheets Precracked Head Sheet Only 3 In-Line Fasteners (Fig. 11)	P2-23	0.199 T 0.200 M 0.199 B	0.202 0.203 0.201	0.030 0.025 0.025	34.80	30.39	204,300	All crack growth in head sheet, at middle fastener. No significant growth at other fasteners.
	P2-24	0.201 T 0.200 M 0.201 B	0.203 0.203 0.202	0.035 0.040 0.035	34.20	29.87	126,000	All growth at end fastener, head sheet only. No significant growth at other fasteners.
	P2-27	0.201 T 0.201 M 0.200 B	0.204 0.203 0.203	0.020 0.025 0.025	34.80	30.39	151,600	All crack growth in head sheet, at middle fastener. No significant growth at other fasteners.
						Average =	160,300	
SWR 2 Sheets Precracked Tail Sheet Only 3 In-Line Fasteners (Fig. 11)	P2-16	0.199 T 0.201 M 0.203 B	0.203 0.206 0.206	0.020 0.030 0.025	34.90	30.48	121,600	Crack growth occurred both in the "tail" and "head" sheets at different locations. Failure at middle fastener of "tail" sheet.
	P2-26	0.200 T 0.199 M 0.199 B	0.204 0.206 0.206	0.025 0.040 0.025	34.90	30.48	184,800	Failed via initiation at location other than precracked hole.
	P2-29	0.200 T 0.202 M 0.199 B	0.206 0.206 0.204	0.025 0.030 0.025	35.00	30.57	140,800	Significant crack growth occurred both in "tail" and "head" sheets at different fastener locations. Failure at middle fastener of "tail" sheet.
						Average =	149,000	
SWR Single Sheet with Back-Up Washers (No Tail Sheet) Precracked 3 In-Line Fasteners (Fig. 12)	P2-21	0.199 T 0.200 M 0.200 B	0.211 0.207 0.208	0.025 0.030 0.025	35.40	30.92	89,700	All crack growth at top fastener. No growth at other fasteners.
	P2-40	0.199 T 0.200 M 0.196 B	0.207 0.208 0.206	0.040 0.035 0.035	35.40	30.92	115,500	All growth at middle fastener. No growth at other fasteners.
	P2-42	0.199 T 0.199 M 0.196 B	0.206 0.207 0.206	0.025 0.030 0.030	35.80	31.00	77,000	All growth at middle fastener. No growth at other fasteners.
						Average =	94,070	
Steel Hi-lok's (clearance fit) 2 Sheets Precracked Head Sheet Only 3 In-Line Fasteners (Fig. 11)	P2-6			0.040 0.030 0.040	35.10	30.65	4850	All crack growth at bottom fastener. No significant growth at other fasteners.
	P2-9			0.035 0.030 0.030	35.10	30.65	6700	All crack growth at bottom fastener. No significant growth at other fasteners.
	P2-18			0.025 0.025 0.030	35.00	30.57	6060	All crack growth at bottom fastener. No significant growth at other fasteners.
1136-027W						Average =	5830	

A group of three specimens, consisting of single sheets with precracked holes containing SWR-driven rivets backed up with washers, were tested. This group had an average crack growth life of 94,070 cycles, about 60% of the average life of the double sheet specimens. The reason for this is not clear. It was initially considered that in the double sheet configuration, load transfer from the cracked to uncracked sheets could possibly extend its life. However, when both head and tail sheets were precracked, the resulting life was nearly identical to the case where only one of the two sheets was precracked. The double sheet specimens, having only one of the sheets precracked, did exhibit longer critical crack lengths than the single sheet specimens, indicating that some unloading of the cracked sheet at the large crack lengths (greater than 0.20 in. or 5.1 mm) occurred. However, the crack propagation life at large cracks lengths is very short, and therefore, insignificant.

Comparison of the uncracked fatigue life (12,000 cycles, Ref. 3, Fig. 20) for the open hole configuration with the uncracked fatigue life for specimens with SWR fasteners, which averages 223,500 cycles (see Table 3), indicates a factor of 19 increase in life for the SWR.

Crack propagation analysis was performed for the open hole specimens, and is presented in Fig. 23 along with test data for three specimens. The agreement between analysis and test here is excellent. Next, crack length versus cycles test data for single and double sheet specimens with SWR-driven rivets is presented in Figs. 24 and 25, respectively. By comparing the test data with the open hole crack propagation analysis, it is seen that the crack propagation life is increased on the average by factors of 30 times for single sheet specimens, to 50 times for double sheet specimens by the installation of rivets with the SWR. In addition, test data for specimens with clearance fit Hi-Loks are also shown in Fig. 25, and it is observed that they increase the specimen life over the open hole configuration by a factor of about two.

A crack propagation analysis of a cracked hole having an SWR-driven rivet was attempted, utilizing the stress intensity solution developed in Section 5. However, the solution (see Fig. 21) indicates that under an applied gross maximum stress of 30.6 ksi (35.0 ksi, net), the stress intensity is reduced to a level below the threshold stress intensity (≈ 3.0 ksi$\sqrt{\text{in.}}$). Hence, no crack growth should occur. Since crack

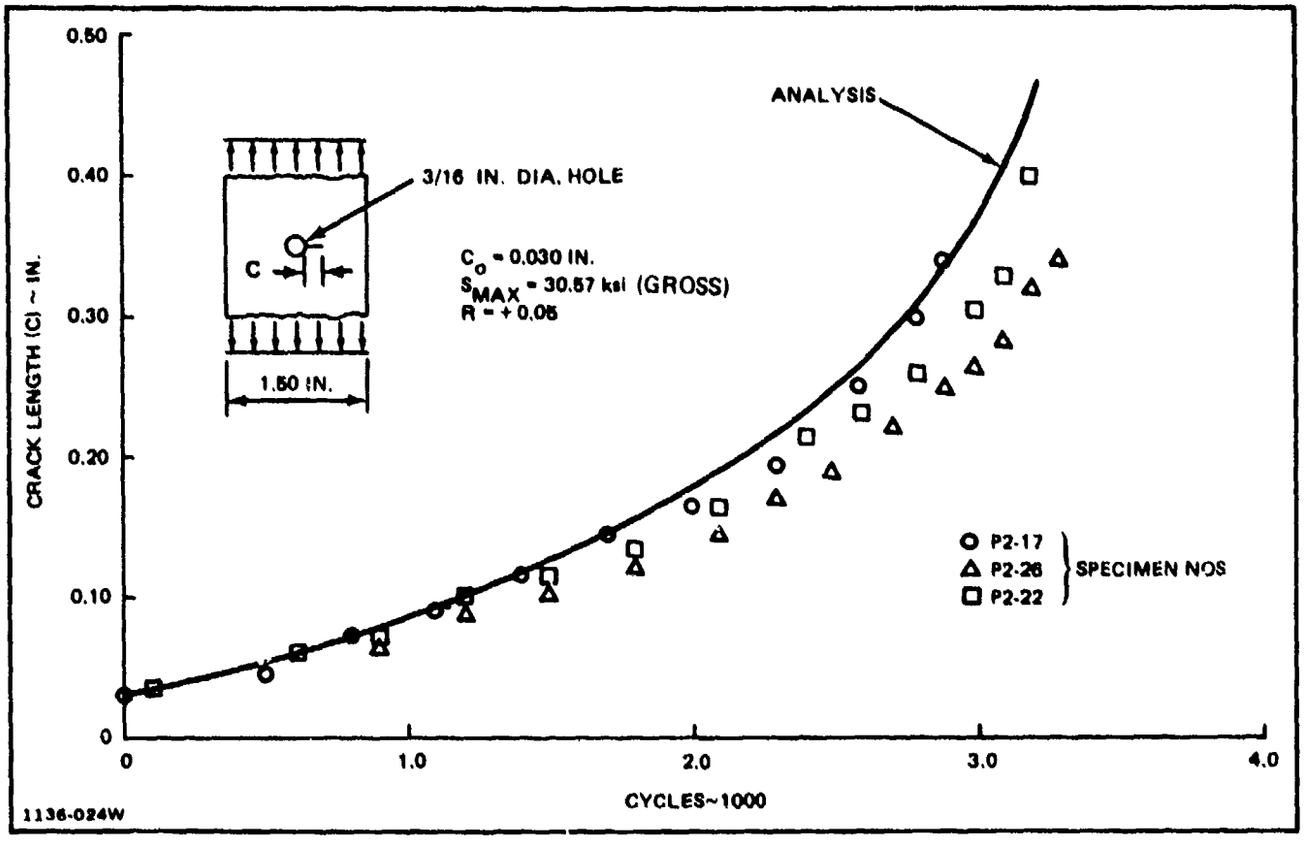

Fig. 23 Constant Amplitude Crack Propagation (Open Hole)

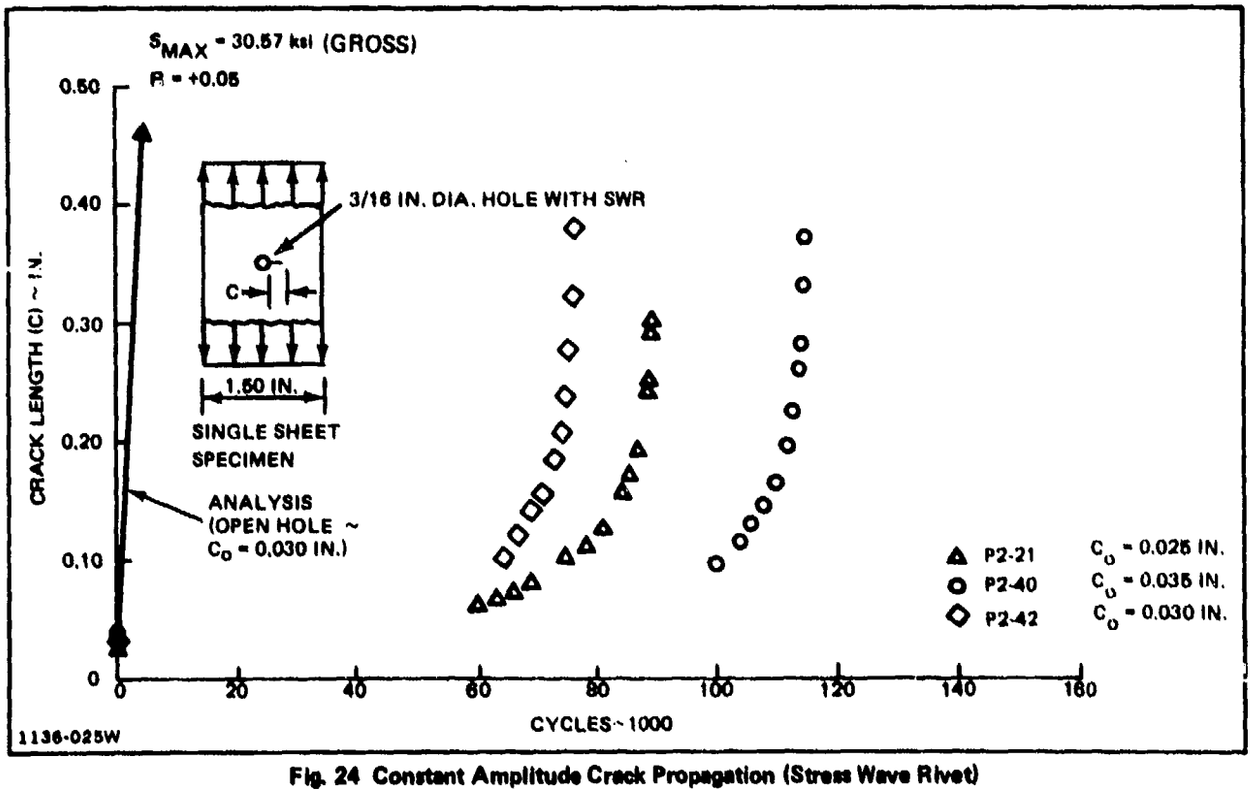

Fig. 24 Constant Amplitude Crack Propagation (Stress Wave Rivet)

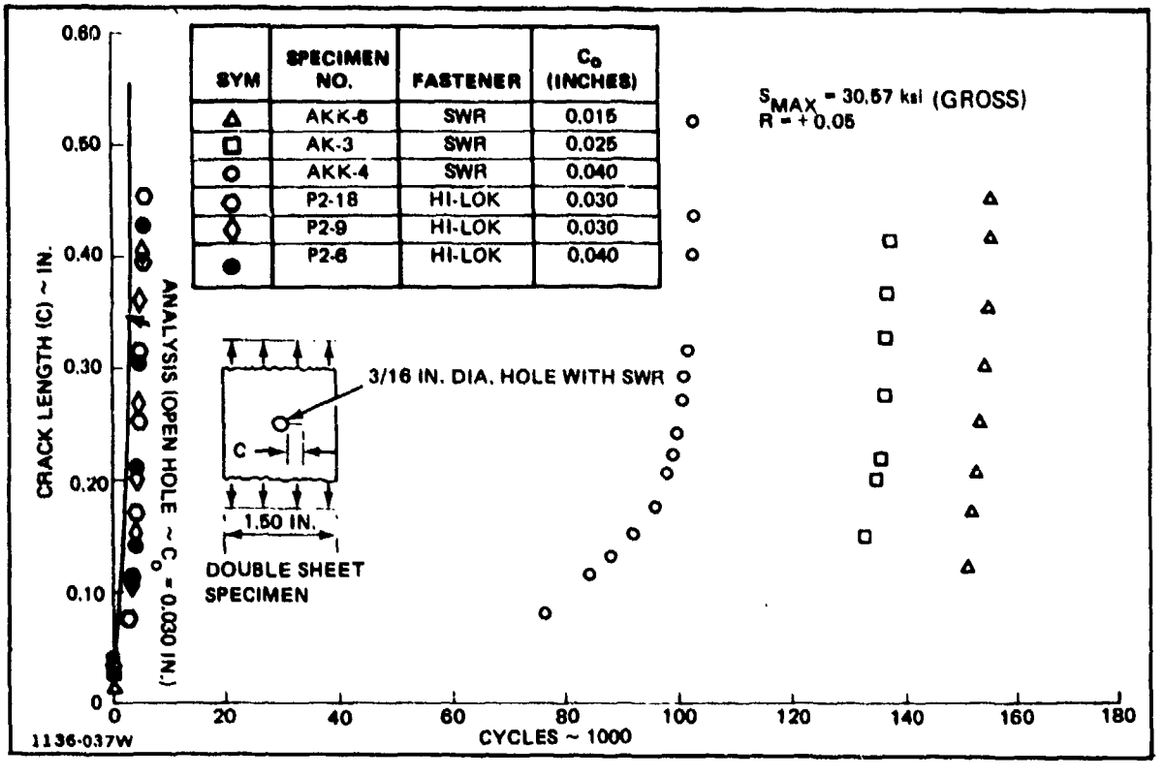

Fig. 25 Constant Amplitude Crack Propagation (Stress Wave Rivet)

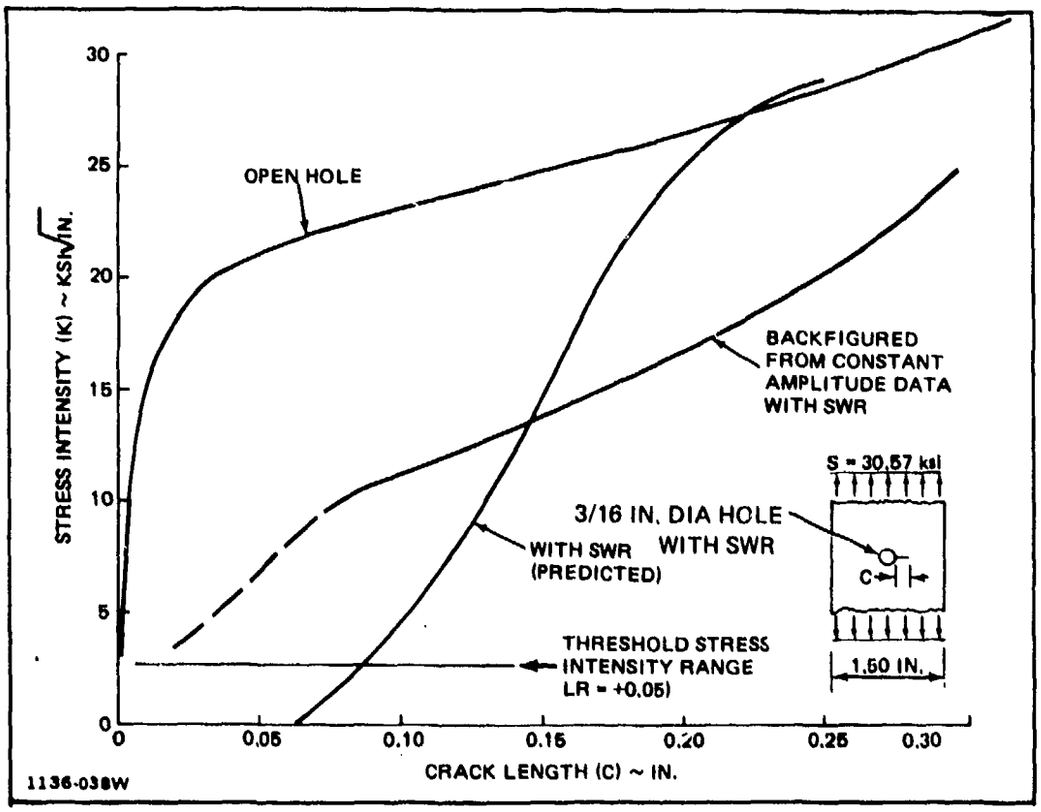

Fig. 26 Stress Intensity

growth did occur, it was decided to backfigure the stress intensity from the fatigue crack propagation rates, in the same manner as Anderson and James (Ref. 11) and Grant and Hinnericks (Ref. 5). The result of this analysis is presented in Fig. 26, where it is noted that the general trends exhibited by the theoretical analysis are found, but that the slope of the test-data-derived stress intensity as a function of crack length is different. The methods yield K's that are significantly different across the range of crack lengths considered with the backfigured results being the more credible. The theoretical analysis attempted here will require further development as discussed later in this report.

The installation of rivets with the SWR produces a residual stress field that retards the crack propagation rate at large distances from the hole. For example, the retarded growth extends out to a distance greater than three radii, as can be seen by examining Fig. 26. Previous studies with coldworked holes (Refs. 5 and 10) indicate that the retarding effect on crack propagation disappears at a crack length to radius ratio (C/R) of about two. The importance of this effect is that the SWR should be able to retard the crack propagation rates with longer initial crack lengths, than can be done by other fastener hole treatments.

SPECTRUM TESTS

A series of tests were performed under fatigue spectrum loading. The test articles are identical to the previously described constant amplitude specimens, except that they are 2.0 in. (50.8 mm) wide instead of 1.5 in. (38.1 mm). The applied fatigue spectrum is a block fighter wing spectrum obtained from Ref. 12, where each block represents 100 flight hours with loads arranged in a low-high-low sequence. The spectrum is presented in Table 4. Fifty-three specimens were tested, and a summary of these test results is presented in Table 5.

A crack propagation analysis was made for a cracked open hole under fatigue spectrum loading at a gross limit stress of 31.68 ksi (218.3 MPa), which in this case is equivalent to a net limit stress of 35.0 ksi (241 MPa). The analysis is presented along with test data in Fig. 27, where good correlation is shown. For an initial crack length (C_o) of 0.035 in. (0.89 mm), the analysis is conservative by about 15%. The Grumman crack closure model, as described in Ref. 13, was used to make the crack propagation prediction shown in Fig. 27, and all subsequent predictions. Analytical predictions and test data for cracked open hole specimens over a range of applied limit stresses are presented in Fig. 28, where it is noted that the analysis is accurate for test data shown. Also shown are test data and predictions for open hole

TABLE 4 F-14 WING SPECTRUM – 15 LAYERS*

Level**	Layer	$\frac{\sigma \text{ Max}}{\sigma \text{ Limit}}$	$\frac{\sigma \text{ Min}}{\sigma \text{ Limit}}$	Cycles / 100 flights
1	1	0.26	0.12	500.
2	2	0.36	0.12	50.
3	3	0.41	-0.18	1.
4	4	0.41	-0.10	14.
5	5	0.41	-0.03	35.
6	6	0.41	0.05	100.
7	7	0.47	0.12	200.
8	8	0.53	0.12	150.
9	9	0.60	0.12	70.
10	10	0.68	0.12	90.
11	11	0.77	0.12	25.
12	12	0.84	0.12	10.
13	13	0.92	0.12	4.
14	14	0.98	0.12	1.
15	15	1.04	0.12	1.
16	14	0.98	0.12	1.
17	13	0.92	0.12	3.
18	12	0.84	0.12	10.
19	11	0.77	0.12	25.
20	10	0.68	0.12	90.
21	9	0.60	0.12	70.
22	8	0.53	0.12	150.
23	7	0.47	0.12	200.
24	6	0.41	0.05	100.
25	5	0.41	-0.03	35.
26	4	0.41	-0.10	13.
27	3	0.41	-0.18	2.
28	2	0.36	0.12	50.
29	1	0.26	0.12	500.

P_{REF} (corresponding to LIMIT Stress/Load) = 1.00

** Designation used in fatigue analysis computer programs

* Ref. NADC – 76383 – 30, (Ref. 12).
Note: 100 flight hour block or 100 flights arranged in low-high low order.
This spectrum is reduced from 212 layers by equivalent exceedances.

1136-026W

TABLE 5 SUMMARY OF SPECTRUM FATIGUE DATA FOR DYNAMICALLY INSTALLED 3/16 IN. DIA A-286 INTERFERENCE FIT FASTENERS IN 2024-T81 ALUMINUM

Type Specimen	Spec. No.	Post Test Fastener Dia. Head Sht/Tail Sht	Initial Crack Length C_o (in.)	Net Limit Stress KSI	Simulated Flight Hrs To Failure	Comments
• Open-Hole • 0.189 in. D in 2.0 in. Wide Sample	OH-1			45	5,800	Failure at middle hole. Significant growth at top hole. No significant growth at bottom hole.
• Three Holes In-Line	OH-2			40.6	11,400	Failure at top hole. No Significant growth at other holes.
• Countersunk open-hole	COH-8			45	6,000	Failure at top hole. Significant growth at all three holes.
• 0.189 in. D in 2.0 in. Wide Sample	COH-10			45	5,500	Failure at middle hole. No significant growth at other holes.
• Three Holes In-Line	COH-1			40	9,900	Failure at top hole. No significant growth at other holes.
	COH-3			40	10,100	Failure at middle hole. No significant growth at other holes.
	COH-2			32	31,500	Failure at top hole. No growth at other holes.
	COH-5			32	32,600	Failure at bottom hole. No growth at other holes.
• Precracked Open-Hole	OHK-2		0.025 0.045 0.050	40	4,400	Failure at bottom hole. No significant growth at top hole.
• 0.189 in. D in 2.0 in. Wide Sample	OHK-3		0.035 0.040 0.045	40	4,400	Significant growth at all three holes. Failure at top hole.
• Three-Holes In-Line	OHK-1		0.040 0.030 0.030	30	14,600	Significant growth at all three holes. Failure at top hole.
	OHK-4		0.035 0.025 0.020	30	14,700	Significant growth at all three holes. Failure at top hole.
	P2-37		T : 0.035 M : 0.040 B : 0.025	35.0	7,500	Significant growth at all three holes. Failure at middle hole.
	P2-41		T : 0.035 M : 0.030 B : 0.035	35.0	7,200	Significant cracks growth at all threeh oles. Failure at bottom hole.
	P2-45		T : 0.025 M : 0.030 B : 1.045	35.0	7,100	Crack growth at all three holes. Failure at bottom hole.
• Stress Wave Riveted (SWR)	1X(1)		0.020/0.030/0.040	45	60,000	No Failure
	P1-1(1)			45	60,000	No Failure
	P1-2(1)		0.020/0.030/0.040	44.3	67,100	Failure at Middle fastener
• Two Sheet Laminate, 2 in. Wide (Except Where Noted	P1-24		0.025/0.030/0.035	36.1	34,600	No Failure
	P1-11		0.020/0.030/0.025	35.8	24,000	No Failure
	P1-18		0.000/0.025/0.025	35.8	24,000	No Failure
	P1-21			35.8	24,000	No Failure
• Three Unloaded In-Line Fasteners	P1-4			35.7	33,200	No FAilure
	P1-16			35.7	25,400	No Failure
	P1-5			35.4	24,000	No Failure
• Precracked "Head" Sheet Only	P1-17			35.4	24,000	No Failure
	P1-20			35.4	24,000	No Failure
	P1-8			35.3	24,000	No Failure
	P1-12			35.3	24,000	No Failure
	P1-13			35.3	24,000	No Failure
	P1-14			35.3	24,000	No Failure
	P1-19			35.3	24,000	No Failure
	P1-15		0.025/0.025/0.015	35.1	24,000	No Failure

Note: (1) Specimen width reduced from 2.0 in. to 1.50 in to accommodate load control equipment.

1136-039W

TABLE 5 SUMMARY OF SPECTRUM FATIGUE DATA FOR DYNAMICALLY INSTALLED 3/16 IN. DIA A-286 INTERFERENCE FIT FASTENERS IN 2024-T81 ALUMINUM (CONT)

Type Specimen	Spec. No.	Post Test Fastener Dia. Head Sht/Tail Sht (in.)	Initial Crack Length C_0 (in.)	Net Limit Stress KSI	Simulated Flight Hrs To Failure	Comments
• SWR • Two Sheet Laminate	P2-13	0.203 0.206 0.203 0.206 0.202 0.206	0.075 0.080 0.080	35.8	28,000	Significant growth at all three fasteners in "head" sheet. Failure at bottom fastener. No Crack in "tail" sheet
• Three Unloaded In-Line Fasteners	P2-14	0.202 0.206 0.201 0.206 0.202 0.206	0.070 0.065 0.080	35.3	22,600	Growth in "head" sheet at all three fasteners. Failure at bottom fastener. No crack in "tail" sheet
• Precracked "Head" Sheet Only • Initial Crack Length Extended to 0.080 in.	P2-43	0.198 0.203 0.199 0.203 0.199 0.203	0.070 0.065 0.080	35.0	28,000	Failure at bottom fastener. No significant growth at other fastener. No crack in "tail" sheet
	P2-44 T M: B	0.199 0.204 0.199 0.204 0.198 0.206	0.065 0.070 0.075	40.1	22,300	Failure at middle fastener. No significant growth at other fasteners.
	P2-47 T M: B	0.198 0.204 0.198 0.202 0.198 0.203	0.065 0.070 0.065	40.1	26,100	Failure at bottom fastener. No significant growth at other fasteners
• SWR, 2.0 in. Wide • Three Unloaded In-Line Fasteners	P2-48 T: M: B:	0.198 0.206 0.198 0.204 0.198 0.204	0.020 0.030 0.026	35.6	24,000	No failure. No visible crack extension
• Single Precracked Sheet with Back-up Washers	P2-49 T M. B:	0.198 0.206 0.198 0.206 0.198 0.206	0.030 0.026 0.030	35.6	24,000	No failure. No visible crack extension
	P2-50 T: M: B			35.5	24,000	No failure. No visible crack extension
• Clearance Fit GB51083-4 Steel Hiloks • 2 Sheet Laminates 2.0 in. wide (except where noted) • Three Unloaded In-Line fasteners • Precracked "Head" Sheet only	HL-4 (1) (P2-3)		0.040 0.045 0.040	44.3	8,100	Significant growth at all three fasteners. Failure at top fastener.
	HL-5 (1) (P2-5)		0.030 0.035 0.026	44.2	9,100	Failure at middle fastener. No significant growth at other fasteners
	HL-1 (P2-4)		0.040 0.040 0.030	39.8	13,200	Significant growth at all three fasteners. Failure at top fastener
	HL-2 P2-8)		0.026 0.020 0.026	40.3	12,500	Significant growth at all three fasteners. Failure at bottom fastener
	HL-3 (P2-7)		0.030 0.035 0.035	35.8	24,200	Significant growth at all three fasteners. Failure at middle fastener
	HL-6 (P2-12)		0.030 0.030	35.2	23,400	Failure at middle fastener. No significant growth at other fasteners
• Clearance Fit GB51083-4 Steel Hiloks, No Clamp-Up	P2-15		T 0.025 M 0.035 B 0.020	35.0	8,400	Failure at middle fastener. No significant growth at other fasteners
• Two Sheet Laminates, 2 in. wide • Three Unloaded In-Line Fasteners	P2-35		T 0.035 M 0.030 B 0.040	35.0	7,600	Significant growth at all three fasteners. Failure at the bottom fastener
• Precracked "Head" Sheet Only	P2-36		T 0.025 M 0.030 B 0.025	35.2	8,400	Crack growth at all three fasteners in head sheet only. Failure at top fastener
• Clearance Fit GB51083-4 Steel Hiloks	P2-30		T 0.030 M: 0.025 B: 0.020	35.5	34,300	Failure at top fastener. No significant growth at other fasteners
• Three Unloaded In-Line Fasteners	P2-39		T 0.035 M: 0.045 B 0.030	35.3	32,100	Crack growth occurred at all three fasteners. Failure at middle fastener
• Single Precracked Sheet With Back-Up Washers, 2 In. Wide	P2-46		T. 0.020 M. 0.020 B: 0.025	35.6	48,300	Cracked growth occurred at all three fasteners. Failure at middle fastener

Note: (1) Specimen width reduced from 2.0 in. to 1.50 in. to accommodate load control equipment.
1136-039W 2.2

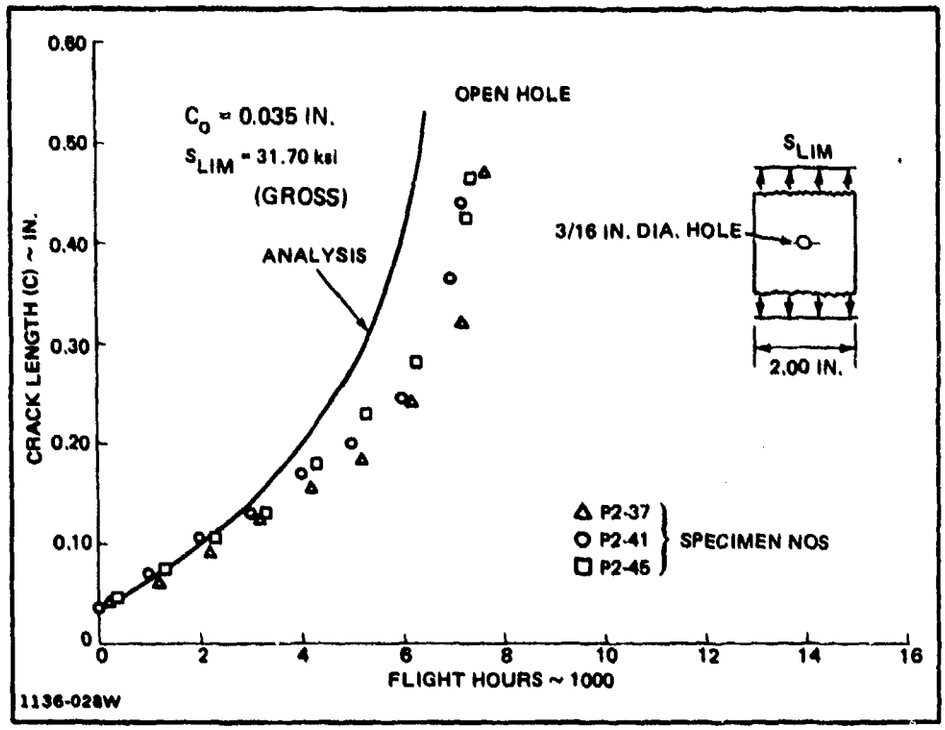

Fig. 27 Spectrum Crack Propagation (Open Hole) 2024-T81 Aluminum

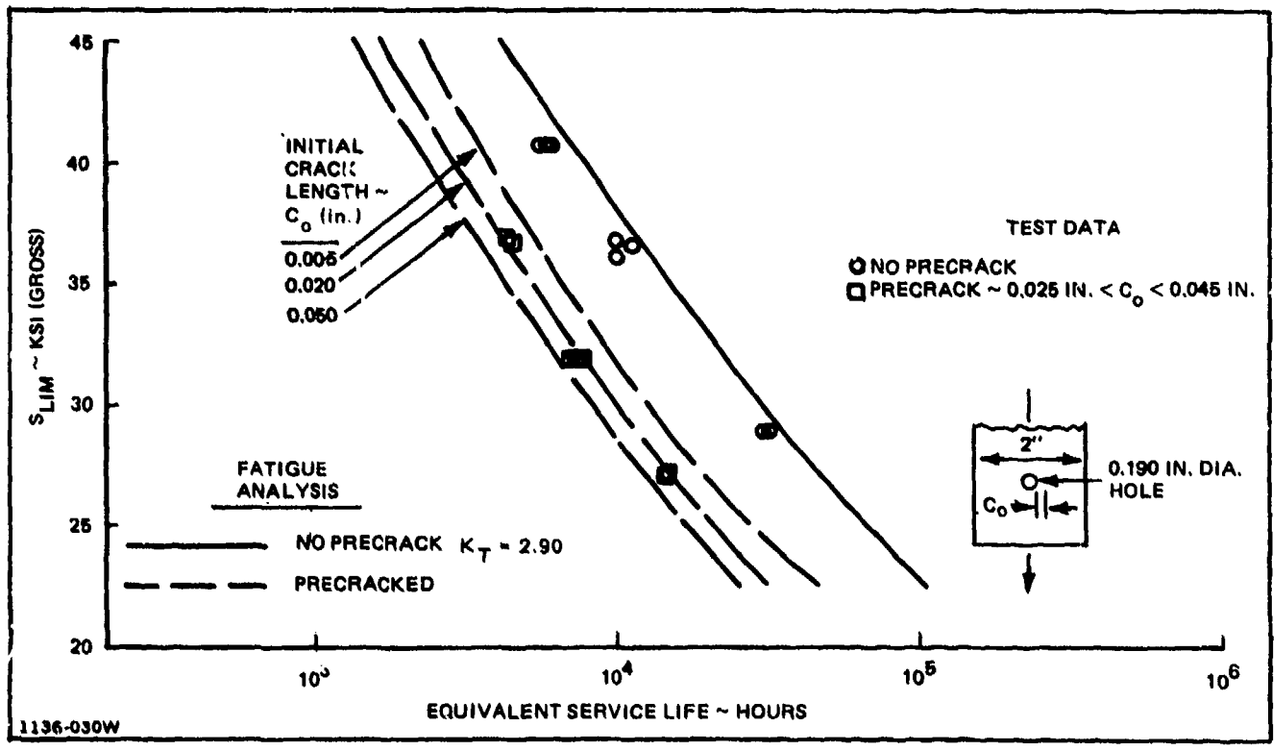

Fig. 28 Spectrum Fatigue Life ~ Open Hole Specimens. 2024-T81 Aluminum

specimens that are not precracked. These predictions are made with cumulative damage calculations based on strain-cycling. Again, good correlation is exhibited.

Fifteen double sheet test articles (Fig. 11) were prepared with stress wave rivets placed in each hole, and with each hole precracked prior to the installation of the rivets. The precracks were located in the head sheets, and were through-the-thickness radial cracks having initial lengths ranging from 0.020 to 0.045 in. All fifteen specimens were tested to 24,000 equivalent flight hours at 31.70 ksi (218.3 MPa) gross limit stress, and no crack growth was detected. Since the fasteners were countersunk, there could have been some crack growth under the rivet head, but the crack length could not have exceeded 0.060 in., since no cracks were observed on the specimen surface. However, four of the specimens were failed statically after completion of the fatigue spectrum cycling. Examination of these specimens subsequent to failure revealed no measureable crack growth during the 24,000 equivalent flight hours of cycling.

An additional three precracked specimens containing rivets driven with the SWR were tested at a gross limit stress of 39.30 ksi (270.8 MPa). Two of the specimens achieved 60,000 hours of fatigue spectrum loads with no cracks detected on the surface, and the tests were terminated. A third specimen failed at 67,100 equivalent flight hours. At this stress level, a precracked open hole configuration would have failed at about 3,000 hours (see Fig. 28), making the increase in life due to the SWR installation a factor of at least 20,

Three test articles were prepared with initial crack sizes of 0.070 in. (1.78 mm) to 0.080 in. (2.03 mm), and were tested under fatigue spectrum loading at 30.57 ksi (210.6 MPa) gross limit stress. These specimens were run to failure. The crack length versus time test data are presented in Fig. 29. Here the life from a 0.080 in. (2.03 mm) initial crack to failure is between 24,000 and 28,000 hours. This is somewhat reasonable, as the total stress intensity at a 0.080 in. (2.03 mm) crack length is about twice what it was at 0.035 in (0.89 mm), and therefore considerably more damage will be done by the spectrum loads. These results indicate that an inital crack of 0.080 in. (2.03 mm) or less could survive for 24,000 flight hours at a gross limit stress or 31.70 ksi (218.2 MPa), and that a 0.050 in. (1.27 mm) initial crack could survive even longer with SWRs installed.

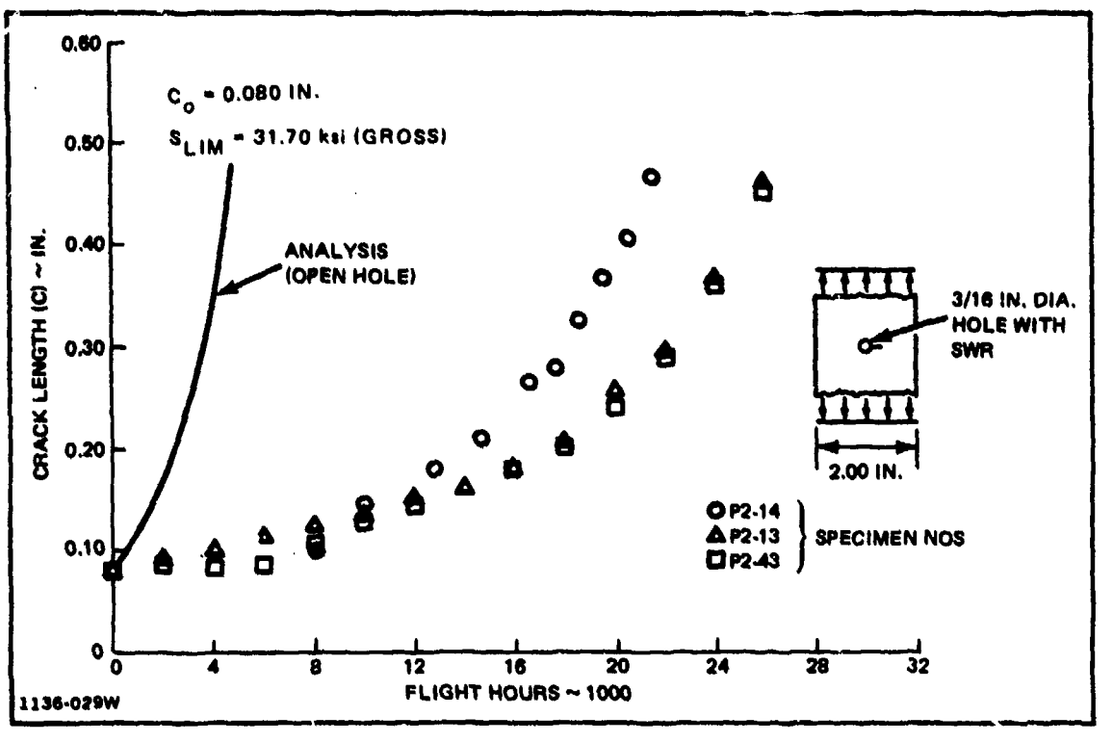

Fig. 29 Spectrum Crack Propagation (Stress Wave Driven Rivet) 2024-T81

Specimens were tested with clearance fit Hi-Lok fasteners, in order to show a comparison of the SWR fasteners with a conventional fastener. Test data at two limit stress levels, 31.68 ksi (218.3 MPa) and 39.30 ksi (270.8 MPa), are presented in Figs. 30 and 31, respectively. Three Hi-Lok specimens were tested without fastener clamp-up. The detrimental effect of lost clamp-up is illustrated in Fig. 30. Clamp-up is not generally considered to be a reliable life enhancement technique for threaded fasteners of this size and type so the unclamped values would likely be used in design. However, against either the clamped or unclamped data the SWRs have an apparent advantage for fatigue or damage tolorant design.

All of the precracked specimen test data are shown in Fig. 32 in order to compare them with each other and with open hole fatigue life predictions. The no clamp-up Hi-Lok data fall between the crack propagation life predictions for initial crack lengths (C_o) of 0.05 in. (1.27 mm) and 0.005 in. (0.127 mm). The average initial crack length for this group of specimens is 0.038 in. (0.965 mm). Test data for Hi-Lok specimens with proper clamp-up tend to lie along the analytical curve for specimens with no precracks. The SWR specimens with initial crack lengths less than 0.045 in. (1.143 mm) are shown in the figure, but are again inconclusive, as they are not tested to failure. One exception is the specimen plotted at a gross limit stress of 38.80 ksi (267.3 MPa) and a life of 67,100 hours. This data point looks considerably superior to both the Hi-Lok and open hole data. Finally, the specimens with SWR-installed rivets with large initial crack lengths ($C_o > 0.065$ in. or $C_o > 1.651$ mm) are shown, and it is observed that they are equal to or better than the Hi-Lok specimens with initial cracks less than 0.045 in. (1.143 mm).

Since the test data presented in Fig 32 does not accurately present the differences between specimens having large and small initial crack lengths, the data was replotted using the product of the gross limit stress (S_{LIM}) and the square root of the initial crack length times π, or, $S_{LIM}\sqrt{\pi C_o}$. The result is shown in Fig. 33, where it is now observed that the SWR data and the Hi-Lok data are separated. Average lines are drawn through these groups of data, and it is noted that for a constant initial crack length and limit stress, the SWR data show about seven times the life of the Hi-Lok data. On this basis, the SWR-installed fasteners are clearly

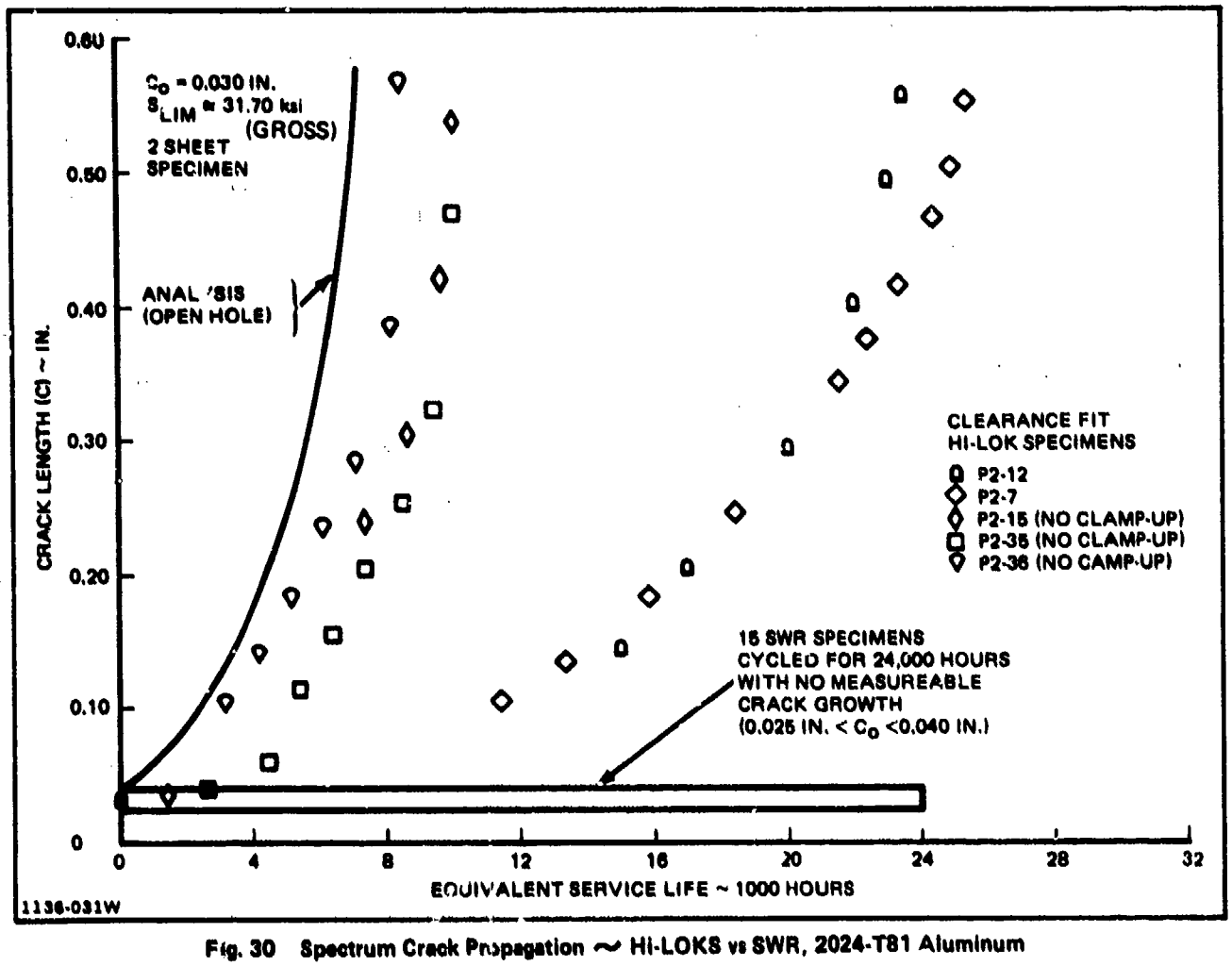

Fig. 30 Spectrum Crack Propagation ~ Hi-LOKS vs SWR, 2024-T81 Aluminum

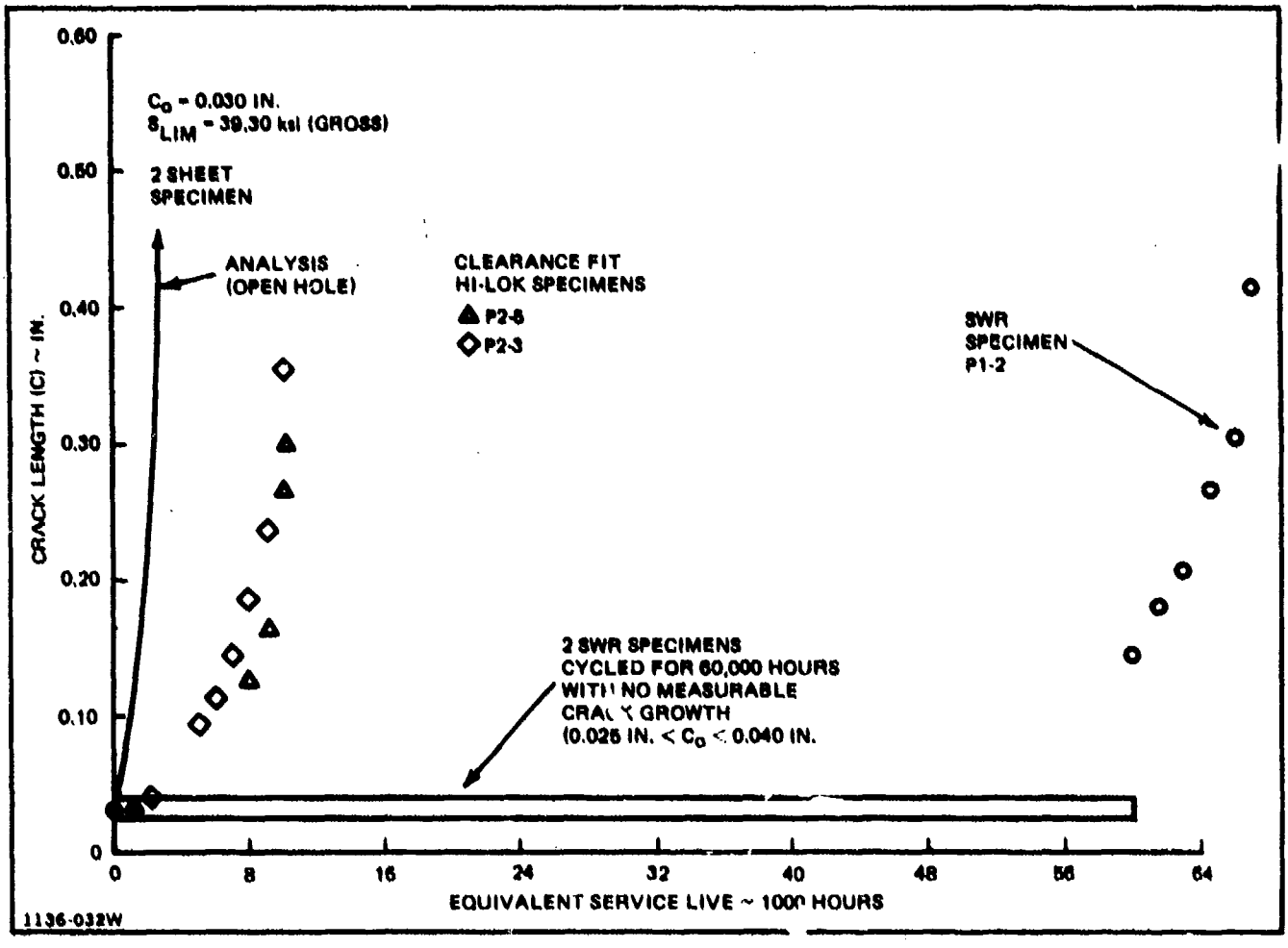

Fig. 31 Spectrum Crack Propagation ~ HI-LOKS vs. SWR, 2024-T81 Aluminum

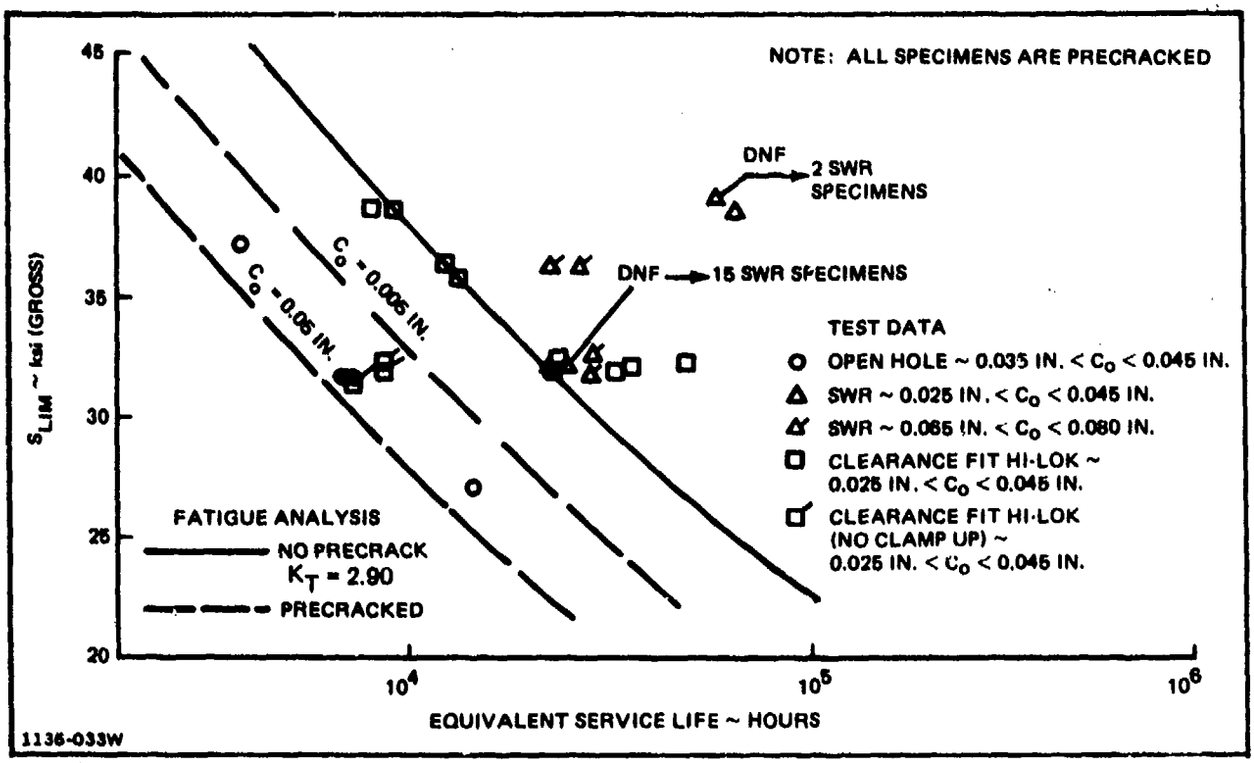

Fig. 32 Spectrum Fatigue Life ~ Stress Wave Rivet Specimens, 2024-T81 Aluminum

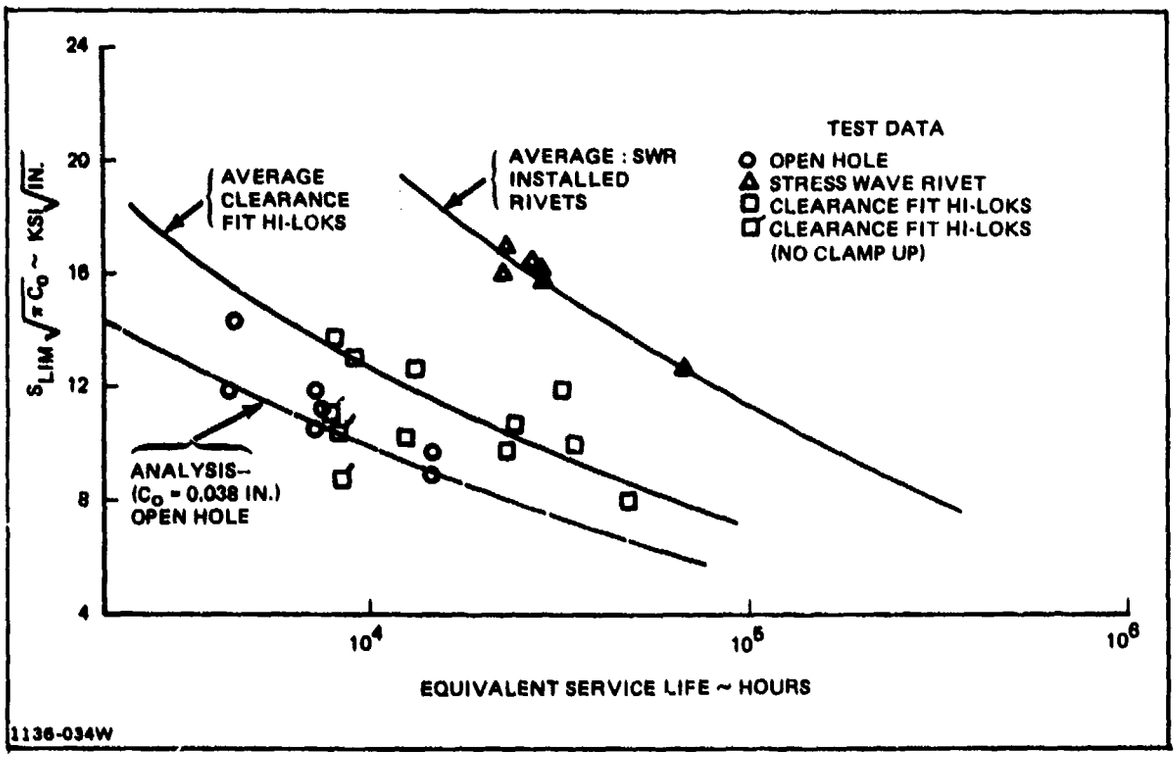

Fig. 33 Effect of Initial Crack Length on Spectrum Fatigue Life 2024-T81 Aluminum

superior to the Hi-Loks. Additionally, the SWR data demonstrates about 17 times the life of the open hole and "no clamp-up" Hi-Lok data. In order to improve the basis for the SWR curve in Fig. 33, some of the SWR specimens tested to only 24,000 hours should be tested to failure. These data will provide points at an $S_{LIM}\sqrt{\pi C_o}$ of about 10.0 KSi $\sqrt{\text{in.}}$ Extrapolation of the SWR curve indicates that the life for these specimens should be about 160,000 hours.

An analytical curve based on an open hole crack propagation analysis is also shown in Fig. 33. The analysis assumes that the initial crack length is 0.038 in. (0.965 mm), an average value for the open hole specimens, and varies the limit stress. The curve shows good correlation with the open hole and "no clamp-up" Hi-Lok test data.

STRESS INTENSITY OF JOINTS RIVETED WITH THE STRESS WAVE RIVETER

The stress intensity calculated for the problem posed here, and previously described in Section 5, does not show agreement with the stress intensity derived from test data using the Anderson and James procedure (Ref 10). The differences could be attributed to the following:

(1) Theoretical stress intensity solutions employing linear superposition, such as performed here and elsewhere (Refs. 7, 14), elastically combine the residual stress field due to plastic straining (cold working) and the remotely applied stress field. These solutions usually predict complete crack arrestment for small crack length. However, experiments here and elsewhere (Refs. 10, 14) show crack growth for small crack lengths, indicating that apparently a relaxation of the residual compressive stress near the hole circumference takes place, permitting crack growth to occur. In the case of non-precracked test articles, crack initiation and crack propagation at small crack lengths takes place similarly.

(2) Residual stresses are calculated for the uncracked configuration, when for most of the specimens, the residual stresses due to the installation of the stress wave driven rivet are introduced into the cracked configuration.

The present effort to predict stress intensity by SWR-produced residual stresses and remotely applied loads is considered an initial attempt and not suitable for design use in its present form. Further effort along these lines will be expanded in the future.

EFFECT OF STRESS WAVE DRIVEN RIVETS ON FIGHTER WING LOWER COVER ALLOWABLE STRESSES

An investigation into the effect of the SWR fasteners on the allowable stresses on a fighter wing lower cover was made, using the fatigue spectrum used in the present SWR study. The structure is assumed to be the riveted sheet and stringer structure shown in Fig. 34, and is made of 2024-T851 aluminum. Design life is assumed to be 12,000 hours, and a scatter factor of two is required. The allowable stresses are presented in Table 6 for a variety of conditions. First, a static allowable limit stress of 37.0 ksi (255 MPa) (limit) is established. Next, a fatigue allowable of 28 ksi (220 MPa) is determined for an effective stress concentration factor of 3.0, i.e., for an uncracked structure. This would be representative of either open holes or a conventional fastener system, and results in a loss of about 14 percent in allowable stress and 11 percent increase in structural weight locally. Here it is assumed that the structural weight changes by 80 percent of the allowable stress change. Use of SWR driven fasteners can increase the fatigue life at the fastener holes sufficiently to raise the allowable stress above the 37.0 ksi static value (see Fig. 32 and consider SWR specimens with S_{LIM} = 39.30 ksi).

Considering a damage tolerant design such as is currently required by the Air Force, and following the slow-crack-growth structure tenets of MIL-A-83444 (Ref. 15), the designer must assume that the structure is initially cracked, and that critical holes have an initial crack length of 0.050 in. (1.27 mm). For a structure thicker than 0.050 in. (1.27 mm), a radial circular corner crack at the hole circumference must be assumed. For open holes or holes with conventional fasteners, and plates thicker than 0.17 in. (4.32 mm), the allowable stress is 23.0 ksi (158 MPa) based on crack propagation life from the initial crack size of 0.050 in. (1.27 mm) to the critical crack size where failure occurs. If SWR fasteners are introduced, the allowable stress will be increased to above 40.7 ksi (280 MPa), and the static allowable stress will govern (see Table 6).

According to specification MIL-A-83444, the use of fatigue enhancing fastener systems such as cold worked holes, interference fits, stress wave driven rivets, etc., requires that an element test program be performed to demonstrate the increased structural life. In addition, the allowable stresses to be used for design must be based on a crack propagation analysis for a crack from the holes in question, assuming a conventional fastener system is installed. However, an initial crack size of 0.005 in. (0.127 mm) is permitted for this analysis. If the analytically determined allowable limit stress is smaller than the test data indicates, the analytical

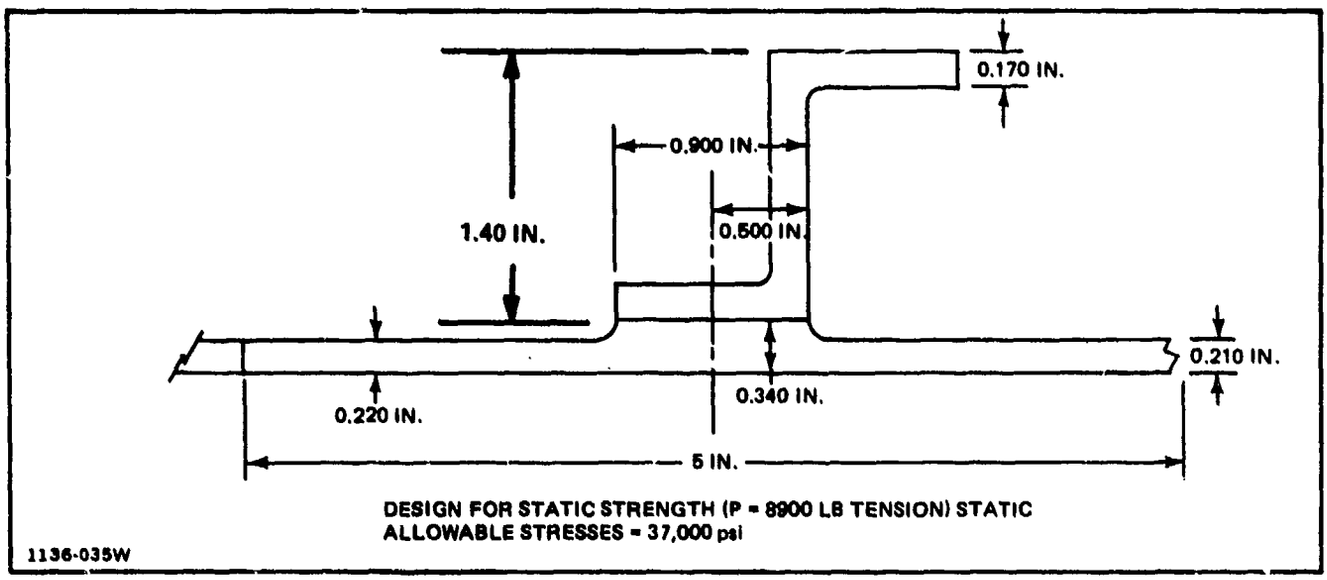

Fig. 34 F-14 Lower Cover Section Simulated in 2024-T851 Aluminum Alloy

TABLE 6 FIGHTER WING LOWER COVER ALLOWABLE STRESSES

2024-T851 ALUMINUM
DESIGN LIFE = 12,000 FLIGHT HOURS

1	2	3	4	5	6
DESIGN CRITERION	CONFIGURATION	FASTENER SYSTEM	INITIAL CRACK LENGTH (IN.)	ALLOWABLE STRESS (Ksi)	WEIGHT PENALTY (PERCENT)
Static Strength	–	–	–	37.0	BASELINE
Fatigue	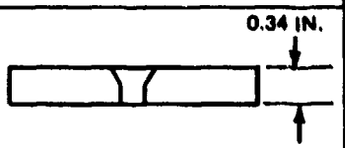	CONVENTIONAL – CLEARANCE	–	28.0	+19.5
		CONVENTIONAL – INTERFERENCE	–	>37.0	0
		SWR	–	>>37.0	0
Damage Tolerance	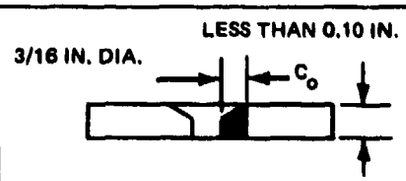	CONVENTIONAL	0.05	20.0	+37.0
		SWR	(*)	25.0	+26.0
		SWR	0.05	>>37.0	0
	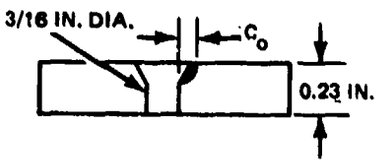	CONVENTIONAL	0.05	23.0	+30.0
		SWR	(*)	28.0	+19.5
		SWR	0.05	>>37.0	0
	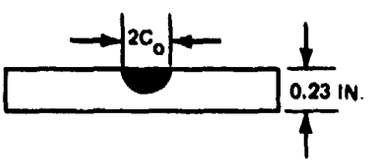	–	0.25	20.0	+37.0
		–	0.10	35.0	+4.3

(*) MIL-A-83444 REQUIRES AN INITIAL CRACK OF 0.005 IN. BE USED WITH CONVENTIONAL CRACK PROPAGATION ANALYSIS FOR CALCULATING DESIGN ALLOWABLE STRESSES.

1136-036W

number must nevertheless be used for design purposes. Therefore, these numbers are also presented in Table 6, and it is noted that their allowable stresses are considerably lower than those demonstrated by test data for the SWR system. For example, consider the case in Table 6 with the corner crack at a hole with SWR-driven rivets. Here, the MIL-A-83444 required analysis provides 28.0 ksi (192 MPa) allowable limit stress for a plate thickness of 0.23 in., whereas the test data generated indicate an allowable stress greater than 40 ksi (275.6 MPa).

Specification MIL-A-83444 also requires that cracks in the structure away from holes must also be considered. For standard non-destructive inspection (NDI) procedures, a semi-circular initial surface crack having a surface length of 0.25 in. (6.35 mm) must be assumed to be present, and the limit allowable stress for this crack will be 20.0 ksi (137 MPa), far less than the static allowable stress. This stress can be increased by reducing the initial crack length to 0.10 in. (2.54 mm) and introducing an NDI demonstration program to establish that the NDI procedures can find the smaller cracks with sufficient reliability. This approach has been implemented in the F-16 program. Using a 0.10 inch initial surface crack length ($2c_o$) increases the allowable stress to 35.0 ksi (241 MPa), and this value will now govern the design. The resulting weight increase is less than 5% over a static design.

The table shows a maximum weight penalty of 37% for a structure with conventional clearance-fit fasteners designed to damage tolerant criteria. Using a stress wave driven rivet fastener system and following the procedures of specification MIL-A-83444 at holes and improved NDI away from holes, the weight penalty is reduced to 19.5%. Furthermore, by using a statistical sample of test data for the SWR fastener treated holes having 0.05 in. (1.27 mm) initial cracks rather than the analytical procedure required by MIL-A-83444, the weight penalty can be reduced to 4.3%. It should also be noted that straight and tapered shank interference fit fastener systems in precracked structures have not been included in the present program.

7. CONCLUSIONS AND RECOMMENDATIONS

The major conclusion of this study is that the installation of stress wave driven rivets is extremely effective in retarding the propagation of cracks from holes. For the case considered, 2024-T81 aluminum specimens subjected to typical fighter wing fatigue spectra and a typical gross limit stress (31.70 ksi or 218.3 MPa), precracked holes were shown experimentally to experience no detectable crack growth during 24,000 equivalent flight hours of spectrum loading. The specimens tested had precracks ranging from 0.020 to 0.045 inches in length, and had A-286 steel stress wave driven rivets installed with 0.006 inch (0.15 mm) radial displacement. There were enough specimens tested under these conditions to provide a valid statistical sample, indicating that this result could be applied to a similar design situation provided that there are no damaging environmental factors present. The crack propagation rates were reduced to the extent that the cracks could be considered to be arrested.

A few specimens identical with the previous group, were tested at a higher gross limit stress (39.30 ksi or 270.8 MPa), and here crack growth retardation from the stress wave driven rivets was sufficient to provide lives in excess of 60,000 equivalent flight hours. This was not a statistical sample but indicates a good potential for application at this stress level. In addition, a few specimens were tested at a gross limit stress of 31.70 ksi (218.3 MPa) but with initial cracks about 0.080 inches (1.78 mm) in length, and here significant crack growth retardation was also exhibited. Lives for this group of specimens averaged about 26,000 equivalent flight hours. It should be noted that for all these cases, the stress wave induced radial displacement was limited to 0.006 in (0.15 mm). A higher radial displacement (say 0.012 in. or 0.30 mm) would have provided higher residual stresses and increased crack growth retardation. The increase in radial displacement will "cold work" the plate material to greater radial distances from the rivet, providing crack growth retardation for longer crack lengths. This would be particularly effective for the case of long initial crack lengths.

Results obtained during the present program indicate that significant weight advantages could be obtained by incorporation of the stress wave riveting system in the manufacture of damage tolerant airframe structures. At the present time the Stress Wave Riveter is not a fully automated production unit, but the system

could easily be incorporated in a Drivematic type riveting machine and used at normal production rates.

Other important recommendations are:

- Partial load transfer specimens riveted with the SWR, should be tested in addition to the zero load transfer specimens evaluated to date.
- Specimens riveted with the SWR should also be tested in controlled corrosive environments to establish whether there is any degradation of the residual stresses.
- Specimens of various thickness and materials should be tested to establish SWR settings before automated applications are made.
- Additional spectrum testing should be performed using load spectra with higher levels of compression loading.
- Higher levels of radial displacement (cold work) and wider variations in hole tolerance should be investigated.
- The repeatability and consistency of the SWR process in a production environment should be examined.

8. REFERENCES

1. Tiffany, C. F., Stewart, R. P., and Moore, T. K., "Fatigue and Stress - Corrosion Test of Selected Fasteners/Hole Processes," ASD-TR-72-111, Jan. 1973.

2. Leftheris, B. P., "Stress Wave Riveter System Analysis," Grumman Research Department Report RE-503, July 1975.

3. Leftheris, B. P., "Advantages of Residual Stresses in Dynamically Riveted Joints," Grumman Research Department Report RE-552, Feb. 1978.

4. Horsch, F. J. and Schwarz, R. C., "Moire Fringe Data Handling System for Application in a Industrial Laboratory," Grumman Engineering Test Operations, presented at the Sixth International Conference for Experimental Stress Analysis, Sept. 1978.

5. Grandt, A. F. Jr., and Hinnerichs, T. D., "Stress Intensity Factor Measurements for Flamed Fastener Holes," U.S. Air Force Materials Laboratory Wright-Patterson Air Force Base, Ohio; presented at the Army Symposium of Solid Mechanics, 10-12 Sept. 1974.

6. Paris, P. C. and Sih, G. C., "Stress Analysis of Cracks," ASTM Special Technical Publication 381, 1970.

7. Grandt, A. F. Jr., "Stress Intensity Factors for Some Thru-Cracked Fastener Holes," Air Force Materials Laboratory, Wright-Patterson Air Force Base, Ohio; presented at the Seventh U. S. National Congress of Applied Mechanics, June 1974.

8. Impellizzeri, L. F. and Rich, D. L., "Spectrum Fatigue Crack Growth in Lugs," - Symposium in Fatigue Crack Growth Under Spectrum Loads, ASTM STP 595, American Society for Testing and Materials, p.p. 320-326, 1976.

9. Bueckner, H. F., "Weight Functions for the Notched Bar," ZAMM 51, 97-109, 1971.

10. Chandawanich, N. and Sharpe, W.N., Jr., "An Experimental Study of Fatigue Crack Initiation and Growth from Coldworked Holes," Engrg. Fract. Mech., vol. 11, pp. 609-620, 1979.

11. James, L.A. and Anderson, W.E., "A Simple Experimental Procedure for Stress Intensity Factor Calibration," J. of Eng. Fracture Mechanics, vol. 1, April 1969, pp. 565-568.

12. Broek, D. and Smith S. H., "Spectrum Loading Fatigue Crack Growth Predictions and Safety Factor Analysis," Report No. NADC-76383-30, Battelle Columbus Laboratories, 24 September 1976.

13. Bell, F.D. and Creager, M., "Crack Growth Analysis for Arbitrary Spectrum Loading," vol. 1, AFFDL-TR-74-129, October 1974.

14. Hsu, T.M., McGee, W.M., and Aberson, J.A., "Extended Study of Flaw Growth at Fastener Holes," AFFDL-TR-77-83, April 1978.

15. MIL-A-83444 (USAF), "Airplane Damage Tolerance Requirements," July 1974.

APPENDIX A
EQUATIONS OF RESIDUAL STRESSES

The residual radial and hoop stresses and strains around an SWR-riveted fastener are given by the following equations (Ref 3).

$$\sigma_r = \left\{ 2K \ln \frac{R_0}{R'} - \frac{E}{1+\mu} \frac{R}{(R')^2} F(t) \right\} + \left\{ 2K \ln \frac{R}{R'} - \frac{E}{1+\mu} \frac{R}{(R')^2} F(t) \right\} \left(\frac{1}{1+C} \right) \left(\frac{R^2}{B^2} - 1 \right) \quad \text{(A-1)}$$

$$\sigma_\theta = \left\{ 2K \left(\ln \frac{R_0}{R'} + 1 \right) - \frac{E}{1+\mu} \frac{R}{(R')^2} F(t) \right\} + \left\{ 2K \left(\ln \frac{R}{R'} + 1 \right) - \frac{E}{1+\mu} \cdot \frac{R}{(R')^2} F(t) \right\} \left(\frac{1}{1+C} \right) \left(\frac{R^2}{B^2} + 1 \right) \quad \text{(A-2)}$$

$$\varepsilon_r = \frac{R^2}{R_0^2} F(t) - \left\{ 2K \ln \frac{R}{R'} - \frac{E}{1+\mu} \frac{R}{(R')^2} F(t) \right\} \left(\frac{1}{1+C} \right) \left(\frac{1+\mu}{E} \right) \left(\frac{R^2}{R_0^2} \right) \quad \text{(A-3)}$$

$$\varepsilon_\theta = -\varepsilon_r \quad \text{(A-4)}$$

where

$K = \frac{\sigma_y}{\sqrt{3}}$ uniaxial yield strength

$F(t)$ = radial displacement (extent of cold work)

$R^1 = \sqrt{\frac{E}{1+\mu} \cdot \frac{R}{K} \cdot F(t)}$

R = radius of hole before riveting

$C = \frac{1+\mu_1}{1+\mu_2} \cdot \frac{E_2}{E_1}$ where subscript 1 refers to the material surrounding the rivet and subscript 2 refers to the material of the rivet

B = reference radius such that $B \gg R$, or riveting of joints equal to the edge distance

R_0 = radius (variable) such that $R < R_0 < B$

The above equations do not include secondary yielding. Reference 3, however, gives the complete derivation.

DISTRIBUTION LIST
Government Activities

	No. of Copies
NAVAIRSYSCOM, AIR-50174 (2 for retention, 2 for AIR-530, 1 for AIR-530215, 1 for AIR-530221C, 2 for AIR-320B).	8
NAVAIRTESTCEN, Patuxent River, Maryland	1
NAVAVNSAFECEN, NAS, Norfolk, Virginia	1
CNAVANTRA, NAS Corpus Christi, Texas	1
CNABATRA, NAS, Pensacola, Florida	1
CNARESTRA, NAS, Glenview, Illinois	1
CNATRA, NAS, Pensacola, Florida	1
NAVAIRSYSCOMREPLANT	1
NAVAIRSYSCOMREPCENT	1
NAVAIRSYSCOMREPAC	1
NAVAIREWORKFAC, NAS, Alameda, California.	1
NAVAIREWORFKAC, NAS, Jacksonville, Florida	1
NAVAIREWORKFAC, NAS, Norfolk, Virginia	1
NAVAIREWORKFAC, NAS, Pensacola, Florida	1
NAVAIREWORKFAC, NAS, Quonset Point, Rhode Island.	1
NAVAIREWORKFAC, NAS, San Diego, California	1
NAVAIREWORKFAC, NAS, Cherry Point, North Carolina	1
COMNAVAIRLANT	1
COMNAVAIRPAC.	1
NWL, Dahlgren, Virginia (Attention Mr. Morton)	1
USAF AFDL, Wright Patterson Air Force Base, OH 4533 (Attention Dr. R. Steward Code)	
USAF Systems Command, WPAFB, Ohio 45433	
Attention FBR	1
Attention FB	1
Attention LLD	1
Attention SEFS	1
Attention FYA	1
Attention LAM	1
Attention FBA	1
Attention LPH	1
USA AMMRC, Watertown, Massachusetts	1
USA APG, Aberdeen, Maryland	1
USA AMRDL, Fort Eustis, VA 23604 (Mr. Berrisford)	1
USA AVSCOM, St. Louis, Missouri (Attention AMSAV-GR)	1
Defense Research and Development Staff, British Embassy Washington, D.C., via NAVAIR (AIR-5302).	1
Canadian Joint Staff, Navy Member Washington, D.C., via NAVAIR (AIR-5302).	1
Technical Advisory, AFIAS-B, Directorate of Aerospace Safety, Norton AFB, California	1
DDC	12
NAVSEASYSCOM, Washington, D.C. 20362 (Mr. C. Pohler, Code 035)	1
NAVSHIPRADCEN, Bethesda, MD 20034 (Attention Mr. A. B. Stavovy 730)	1

DISTRIBUTION LIST (cont)

	No. of Copies
Aircraft Industry	
Bell Aerosystems Co., Buffalo, New York 14205	1
Bell Helicopter Co., Fort Worth, Texas 76101.	1
Boeing Co., Airplane Div., Seattle, Washington 98124 (Mr. T. Porter and Mr. Joseph Phillips)	1
Boeing Co., Airplane Div., Wichita, Kansas 67210	1
Boeing Co., Vertol Div., Phila., Pa. 19142	1
McDonnell Douglas Aircraft Corp., Aircraft Div., Long Beach, California 90801	1
General Dynamics/Convair, San Diego, California 92112	1
General Dynamics Corp., Fort Worth, Texas 76101	1
Goodyear Aerospace Corp., Akron, Ohio 44305	1
Grumman Aerospace Corp., Bethpage, Long Island, New York 11714 (Mr. B. Beal and Dr. B. Leftheris)	1
Aircraft-Missiles Div., Fairchild-Hiller Corp., Hagerstown, Maryland 21740	1
Kaman Aircraft Corp., Bloomfield, Connecticut 06002	1
Lockheed Aircraft Corp., Lockheed-California Co., Burbank, California 91503	1
Lockheed Aircraft Corp., Lockheed-Georgia Co., Marietta, Georgia 30061	1
LTV Aerospace Corp., Dallas, Texas 75222.	1
Martin Co., Baltimore Md. 21203	1
McDonnell Douglas Aircraft Corp., St. Louis, Missouri 63166	1
Rockwell International, Columbus Aircraft Div, Columbus OH 43216 (Mr. O. Acker)	1
Rockwell International, Los Angeles, CA. 90053 (Mr. G. Fitch)	1
Northrop Corp., Aircraft Div., Hawthorne, California 90250	1
Republic Aviation Div., Fairchild-Hiller Corp., Farmingdale, Long Island, New York 11735	1
Sikorsky Aircraft Co., Stratford, Connecticut 06497	1
Standard Pressed Steel Corp., Jenkintown, PA 19046 (Mr. Garreth)	
Research Organizations	
Drexel University, Philadelphia, PA 19104 (Attention Dr. H. Harris)	
Hdqtrs., R&T Div., AFSC, Bolling AFB, District of Columbia 20332.	1
Office of Aerospace Research, Arlington, Virginia 22209	1
FAA (FS-120), Washington, D.C. 20553.	1
Scientific and Technical Information Facility, College Park, Maryland 20740 (NASA Rep.)	2
Administrator, NASA, Washington, D.C. 20546	1
NASA-Langley Research Center, Materials Division Hampton, VA 23365 (Mr. H. F. Hardrath)	1
National BuStds, Washington, D.C. 20234	1
Office of Naval Research, Washington, D.C. 20362 Dr. N. Perrone).	1
Director, Naval Research Lab, Washington, D.C. 20390	1
Midwest Research Institute, Kansas City, Missouri 64110	1
University of Illinois, Urbana, Illinois 61803 (Prof. T. J. Dolan and Prof. J. Morrow)	1 each

DISTRIBUTION LIST (cont)

	No. of Copies
University of Kansas, Lawrence, Kansas 66044.	1
University of Michigan, Ann Arbor, Michigan 48105	1
University of Minesota, Mineapolis, Minnesota 55455	1
Alcoa, Alcoa Labs, Alcoa Center PA 15069 (Mr. J. G. Kaufman). . . .	1
LeHigh University, Bethlehem, PA 18015 (Prof. G. C. Sih).	1
University of Dayton Research Institute 300 College Park Dayton, OH 46469 (Dr. J. Gallagher).	1
Belfour Stulen, Inc., Traverse City, Michigan 49684	1
Cornell Aero. Lab, Buffalo, New York 14221	1
Metals & Ceramics Information Center, Battelle, Columbus Laboratories, Columbus, Ohio 43201	1
NASA, Lewis Research Center, Cleveland, OH 44153 (Tech Library) . . .	1
Naval Postgraduate School, Monterey, California 93940 (Prof. Lindsey).	1

Government Agencies

ASD, WPAFB, OH 45433 (Attn: Dr. J. Goodman).	1
AFFDL, WPAFB, OH 45433 (Attn: Mr. R.M. Bader)	1
NASA, Langley Research Center, Hampton, VA 23665 (Attn: Mr. H. Hardrath).	1
USAAVRDC, Applied Tech. Lab, Fort Eustis, VA 23604 (Attn: Mr. H. Reddich, Jr.).	1
British Defence Staff, Defence Equipment Staff, British Embassy, 3100 Massachusetts Ave., N.W., Wash. D.C. 20008 (Attn: Mr. F.S. Wood).	1

Distribution Outside United States

National Aero. Establishment, National Research Council, Montreal Road, Ottawa KIA OR6, Ontario, Canada Attn: Mr. John Dunsby.	1
Royal Aircraft Establishment, Farnsborough, Hants GU146TD, England Structures Department (Attn: Messrs: P. Guyett, R. Maxwell, W. Kirkby).	3
Aeronautical Research Labs Structures Division Box 4331 PO, Melbourne, Victoria 3001 Austrailia (Attn: Dr. Alfred Payne)	1
Defence Scientific Establishment HMNZ Dockyard, Aukland 9, New Zealand (Attn: Mr. H. Levinsohn) .	1